

# UNCLASSIFIED

AD NUMBER
ADB250216
NEW LIMITATION CHANGE
TO Approved for public release, distribution unlimited
FROM Distribution authorized to U.S. Gov't. agencies only; Proprietary Info; Aug 99 Other requests shall be referred to USAMRMC, Ft. Detrick, MD 21702-5012
AUTHORITY
USAMRMC ltr, dtd 15 May 2003

THIS PAGE IS UNCLASSIFIED

AWARD NUMBER DAMD17-98-1-8171

TITLE: Epidermal Growth Factor Receptor Overexpression as a Target  
for Auger Electron Radiotherapy of Breast Cancer

PRINCIPAL INVESTIGATOR: Raymond M. Reilly, Ph.D.

CONTRACTING ORGANIZATION: The Toronto Hospital  
Toronto, Ontario M5G 2C4 Canada

REPORT DATE: August 1999

TYPE OF REPORT: Annual

PREPARED FOR: U.S. Army Medical Research and Materiel Command  
Fort Detrick, Maryland 21702-5012

DISTRIBUTION STATEMENT: Distribution authorized to U.S. Government agencies only (proprietary information, Aug 99). Other requests for this document shall be referred to U.S. Army Medical Research and Materiel Command, 504 Scott Street, Fort Detrick, Maryland 21702-5012.

The views, opinions and/or findings contained in this report are those of the author(s) and should not be construed as an official Department of the Army position, policy or decision unless so designated by other documentation.

20000105 062

## NOTICE

USING GOVERNMENT DRAWINGS, SPECIFICATIONS, OR OTHER DATA INCLUDED IN THIS DOCUMENT FOR ANY PURPOSE OTHER THAN GOVERNMENT PROCUREMENT DOES NOT IN ANY WAY OBLIGATE THE U.S. GOVERNMENT. THE FACT THAT THE GOVERNMENT FORMULATED OR SUPPLIED THE DRAWINGS, SPECIFICATIONS, OR OTHER DATA DOES NOT LICENSE THE HOLDER OR ANY OTHER PERSON OR CORPORATION; OR CONVEY ANY RIGHTS OR PERMISSION TO MANUFACTURE, USE, OR SELL ANY PATENTED INVENTION THAT MAY RELATE TO THEM.

### LIMITED RIGHTS LEGEND

Award Number: DAMD17-98-1-8171

Organization: The Toronto Hospital

Those portions of the technical data contained in this report marked as limited rights data shall not, without the written permission of the above contractor, be (a) released or disclosed outside the government, (b) used by the Government for manufacture or, in the case of computer software documentation, for preparing the same or similar computer software, or (c) used by a party other than the Government, except that the Government may release or disclose technical data to persons outside the Government, or permit the use of technical data by such persons, if (i) such release, disclosure, or use is necessary for emergency repair or overhaul or (ii) is a release or disclosure of technical data (other than detailed manufacturing or process data) to, or use of such data by, a foreign government that is in the interest of the Government and is required for evaluational or informational purposes, provided in either case that such release, disclosure or use is made subject to a prohibition that the person to whom the data is released or disclosed may not further use, release or disclose such data, and the contractor or subcontractor or subcontractor asserting the restriction is notified of such release, disclosure or use. This legend, together with the indications of the portions of this data which are subject to such limitations, shall be included on any reproduction hereof which includes any part of the portions subject to such limitations.

THIS TECHNICAL REPORT HAS BEEN REVIEWED AND IS APPROVED FOR PUBLICATION.

Patricia Madron

12/13/99

# REPORT DOCUMENTATION PAGE

Form Approved  
OMB No. 0704-0188

Public reporting burden for this collection of information is estimated to average 1 hour per response, including the time for reviewing instructions, searching existing data sources, gathering and maintaining the data needed, and completing and reviewing the collection of information. Send comments regarding this burden estimate or any other aspect of this collection of information, including suggestions for reducing this burden, to Washington Headquarters Services, Directorate for Information Operations and Reports, 1215 Jefferson Davis Highway, Suite 1204, Arlington, VA 22202-4302, and to the Office of Management and Budget, Paperwork Reduction Project (0704-0188), Washington, DC 20503.

1. AGENCY USE ONLY (Leave blank)		2. REPORT DATE August 1999	3. REPORT TYPE AND DATES COVERED Annual (1 Jul 98 - 1 Jul 99)
4. TITLE AND SUBTITLE Epidermal Growth Factor Receptor Overexpression as a Target for Auger Electron Radiotherapy of Breast Cancer			5. FUNDING NUMBERS DAMD17-98-1-8171
6. AUTHOR(S) Raymond M. Reilly, Ph.D.			
7. PERFORMING ORGANIZATION NAME(S) AND ADDRESS(ES) The Toronto Hospital Toronto, Ontario M5G 2C5 Canada			8. PERFORMING ORGANIZATION REPORT NUMBER
9. SPONSORING / MONITORING AGENCY NAME(S) AND ADDRESS(ES) U.S. Army Medical Research and Materiel Command Fort Detrick, Maryland 21702-5012			10. SPONSORING / MONITORING AGENCY REPORT NUMBER
11. SUPPLEMENTARY NOTES			
12a. DISTRIBUTION / AVAILABILITY STATEMENT Distribution authorized to U.S. Government agencies only (proprietary information, Aug 99). Other requests for this document shall be referred to U.S. Army Medical Research and Materiel Command, 504 Scott Street, Fort Detrick, Maryland 21702-5012.			12b. DISTRIBUTION CODE
13. ABSTRACT (Maximum 200 words) Overexpression of the epidermal growth factor receptor (EGFR) occurs in a high proportion of estrogen receptor-negative and hormone-resistant breast cancers. Our objective is to construct a human epidermal growth factor (hEGF)-immunoglobulin (CH1) fusion protein to deliver the Auger electron emitting radionuclide, <sup>111</sup> In into the cytoplasm and nucleus of breast cancer cells for targeted radiotherapy. The gene for hEGF was amplified from plasmid pADH59 by the polymerase chain reaction (PCR) and inserted into pASK84 which contains the genes for CH1 and CK of IgG1. The hEGF-CH1 gene was amplified from pASK84 by PCR and inserted into expression plasmid pGEX2T for expression in E. coli. Conditions for expression were optimized. The fusion protein was isolated using native or denaturing conditions. SDS-PAGE and Western blot analysis showed a pure protein with the expected molecular size (M <sub>r</sub> 18 kDa). Flow cytometry against MDA-MB-468 cells and ELISA against purified EGFR demonstrated that the hEGF-CH1 protein exhibits preserved receptor-binding properties. Biodistribution studies in athymic mice with MDA-MB-468 breast cancer xenografts are in progress. In conclusion, we successfully generated a recombinant hEGF-CH1 fusion protein of high purity which exhibits preserved receptor-binding properties.			
14. SUBJECT TERMS Breast Cancer, radiotherapy, Auger electrons, epidermal growth factor receptor			15. NUMBER OF PAGES 62
			16. PRICE CODE
17. SECURITY CLASSIFICATION OF REPORT Unclassified	18. SECURITY CLASSIFICATION OF THIS PAGE Unclassified	19. SECURITY CLASSIFICATION OF ABSTRACT Unclassified	20. LIMITATION OF ABSTRACT Limited

## FOREWORD

Opinions, interpretations, conclusions and recommendations are those of the author and are not necessarily endorsed by the U.S. Army.

\_\_\_\_ Where copyrighted material is quoted, permission has been obtained to use such material.

\_\_\_\_ Where material from documents designated for limited distribution is quoted, permission has been obtained to use the material.

\_\_\_\_ Citations of commercial organizations and trade names in this report do not constitute an official Department of Army endorsement or approval of the products or services of these organizations.

✓ In conducting research using animals, the investigator(s) adhered to the "Guide for the Care and Use of Laboratory Animals," prepared by the Committee on Care and use of Laboratory Animals of the Institute of Laboratory Resources, national Research Council (NIH Publication No. 86-23, Revised 1985).

✓ For the protection of human subjects, the investigator(s) adhered to policies of applicable Federal Law 45 CFR 46.

\_\_\_\_ In conducting research utilizing recombinant DNA technology, the investigator(s) adhered to current guidelines promulgated by the National Institutes of Health.

\_\_\_\_ In the conduct of research utilizing recombinant DNA, the investigator(s) adhered to the NIH Guidelines for Research Involving Recombinant DNA Molecules.

\_\_\_\_ In the conduct of research involving hazardous organisms, the investigator(s) adhered to the CDC-NIH Guide for Biosafety in Microbiological and Biomedical Laboratories.



PI - Signature

July 23, 1999

Date

## **TABLE OF CONTENTS**

Front Cover .....	1
Standard Form (SF) 298 .....	2
Foreword .....	3
Table of Contents .....	4
Introduction .....	5
Research Conducted .....	5
Construction of an hEGF-C <sub>H</sub> 1 expression vector .....	5
Optimization of Expression Conditions .....	7
Purification of hEGF-C <sub>H</sub> 1 Protein under Native Conditions .....	8
Evaluation of Receptor-Binding Properties .....	9
Purification of the hEGF-C <sub>H</sub> 1 Protein using Denaturing Conditions .....	11
Future Work .....	12
Key Research Accomplishments .....	12
Reportable Outcomes .....	12
Manuscripts and Abstracts .....	12
Presentations .....	13
Patents Applied .....	13
Other Funding Applied .....	13
Conclusions .....	13
References .....	14
Appendices .....	15
Indium-111 Labelled EGF is Selectively Radiotoxic to Human Breast Cancer Cells Overexpressing the EGFR .....	16
A Comparison of EGF and Monoclonal Antibody 528 Labeled with Indium-111 for Imaging Breast Cancer .....	39
Production of a Human Epidermal Growth Factor (hEGF)- Immunoglobulin (C <sub>H</sub> 1) Fusion Protein for Targeting Human Breast Cancer .....	61

## **INTRODUCTION**

Overexpression of the epidermal growth factor receptor (EGFR) occurs in a high proportion of estrogen receptor-negative and hormone-resistant breast cancers (1). We have previously shown (2) that human epidermal growth factor (hEGF) conjugated to the Auger electron-emitting radionuclide, indium-111 ( $^{111}\text{In}$ ) is specifically bound by breast cancer cells overexpressing the EGFR, is internalized by the cells and is translocated to the cell nucleus. The proximity of the Auger electrons emitted from  $^{111}\text{In}$  deposits high doses of radiation in the cell nucleus which damage chromosomal DNA, killing the cells. The low energy and corresponding subcellular range of the Auger electrons restricts the cytotoxicity of  $^{111}\text{In}$ -hEGF however to cells which specifically bind and internalize the radiolabelled growth factor. As a result, there is minimal radiotoxicity to most normal tissues, which exhibit only very low levels of EGFR expression.  $^{111}\text{In}$ -hEGF is a promising agent for targeted radiotherapy of hormone-resistant advanced breast cancer but its rapid elimination by renal excretion results in relatively low accumulation in breast cancer xenografts in athymic mice (3). The objective of this project is to construct a recombinant fusion protein consisting of hEGF and the  $\text{C}_\text{H}1$  domain of  $\text{IgG}_1$  ( $M_r$  18-36 kDa) which will exhibit slower blood clearance and improved tumour uptake for targeted radiotherapy of breast cancer. The hEGF- $\text{C}_\text{H}1$  fusion protein will be radiolabelled with  $^{111}\text{In}$  and tested for cytotoxicity against breast cancer cells *in vitro* and against breast cancer xenografts hosted in athymic mice *in vivo*. In this first year report, we describe research conducted to construct the recombinant hEGF- $\text{C}_\text{H}1$  prokaryotic expression vector and express, purify and test the fusion protein for binding against MDA-MB-468 human breast cancer cells (4).

## **RESEARCH CONDUCTED**

*Task 1: Construction of a novel fusion protein of a single, constant domain of IgG ( $\text{C}_\text{H}1$ ) and hEGF.*

### **1. Construction of an hEGF- $\text{C}_\text{H}1$ expression vector**

A recombinant prokaryotic hEGF- $\text{C}_\text{H}1$  expression vector was constructed (Fig. 1) and successfully used to produce an hEGF- $\text{C}_\text{H}1$  fusion protein in *E. coli*. The hEGF gene was amplified from plasmid pADH59 (obtained from the American Type Culture Collection, ATCC) by the polymerase chain reaction (PCR) using oligonucleotide primers containing the restriction sites *Pst* I and *Bst* EI. The amplified hEGF gene was then ligated into plasmid pASK84 (obtained from ATCC) containing the  $\text{C}_\text{H}1$  and  $\text{C}_\text{K}$  domains of  $\text{IgG}_1$  at the *Pst* I and *Bst* EI restriction sites. The hEGF and  $\text{C}_\text{H}1$  DNA was sequenced to ensure that they were in the correct reading frame. The recombinant hEGF- $\text{C}_\text{H}1$  gene was then amplified from pASK84 by PCR using oligonucleotide primers containing the restriction sites *Eco* R1 and *Bam* H1 with/without an intervening DNA sequence

encoding a flexible polypeptide linker [(GGGGS)<sub>3</sub>] and ligated into plasmid pGEX2T (Amersham-Pharmacia Biotech) to produce the final expression plasmid pJW4. The expression plasmid, pJW4 expresses the hEGF-C<sub>H</sub>1 protein fused to glutathione S-transferase (GST) under the control of the Lac I<sup>q</sup> promoter induced by isopropyl-b-D-thiogalactopyranoside (IPTG). The DNA sequence of the final hEGF-C<sub>H</sub>1 construct was confirmed (Fig. 2).

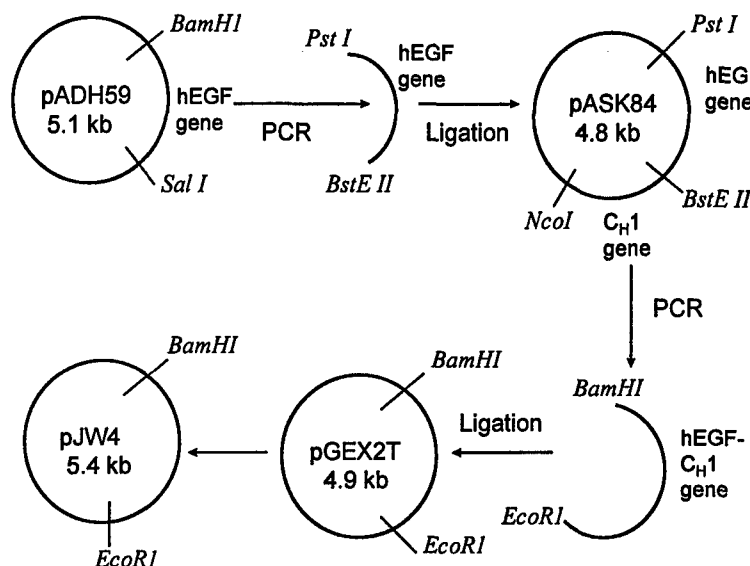


Fig. 1. Scheme for construction of the hEGF-C<sub>H</sub>1 expression vector.

<u>BamHI</u>																				63
gga tcc aac tct gat tcc gaa tgc ccg ctg tct cat gac ggt tac tgc ctg cat gat ggc gta																				gta
G S N S D S E C P L S H D G Y C L H D G V																				V
tgc atg tac atc gaa gct ctg gac aaa tac gca tgc aac tgt gtt gta ggt tac atc ggc gaa																				126
C M Y I E A L D K Y A C N C V V G Y I G E																				E
cgt tgc cag tat cgc gac ctg aaa tgg tgg gaa ctg cgt ggt ggc ggt ggc tgc ggc ggt																				189
R C Q Y R D L K W E L R G G G G S G G G																				G
ggg tgc ggt ggc ggc gga tct acg gtc acc gtc tcc tca gca aag acc act cct ccg tct gtt																				252
G S G G G G S T V T V S S A K T T P P S V																				V
tac cct ctg gct cct ggt tct gcg gct cag act aac tct atg gtg act ctg gga tgc ctg gtc																				315
Y P L A P G S A A Q T N S M V T L G C L V																				V
aag ggc tat ttc cct gag cca gtg aca gtg acc tgg aac tct gga tcc ctg tcc agc ggt gtg																				378
K G Y F P E P V T V T W N S G S L S S G V																				V
cac acc ttc cca gct gtc ctg caa tct gac ctc tac act ctg agc agc tca gtg act gtc ccc																				441
H T F P A V L Q S D L Y T L S S S V T V P																				P
tcc agc acc tgg ccc agc gag acc gtc acc tgc aac gtt gcc cac ccg gct tct agc acc aaa																				504
S S T W P S E T V T C N V A H P A S S T K																				K
ggt gac aag aaa atc gta ccg cgc gac tgc cat cac cac cat cac cat gaa ttc																				567
V D K K I V P R D C H H H H H H E F																				

Fig. 2. Confirmed DNA and corresponding amino acid sequence for hEGF-C<sub>H</sub>1 insert in pJW4 showing hEGF (blue), peptide linker (red) and C<sub>H</sub>1 (green) domains of the fusion protein.

## 2. Optimization of expression conditions

The expression plasmid pJW4 was transfected into *E. coli* (BL-21). Different conditions were evaluated to optimize the expression of the hEGF-C<sub>H</sub>1 fusion protein: 1) incubation temperature (30 °C or 37 °C), 2) IPTG concentration (0-1 mM) and 3) induction time (0-4 hours). Total bacterial protein was isolated from inclusion bodies in cell culture lysates using 8 M urea. The expression yield of the hEGF-C<sub>H</sub>1 fusion protein was measured by 1) assaying for total protein using a BioRad colorimetric protein assay normalized for endogenous bacterial protein synthesis and 2) by Western blot specific for the hEGF-C<sub>H</sub>1 fusion protein using a polyclonal anti-hEGF antibody. The protein assay demonstrated that a higher protein yield was obtained at 37 °C compared to 30 °C and that an induction time of 3-4 hours was required (Table I). The Western blot also confirmed that a higher yield of the fusion protein was obtained at 37 °C and with a 4 hour induction time (Fig. 3).

**Table I.** Effect of Induction Time and Temperature on Yield of the hEGF-C<sub>H</sub>1 Protein.

IPTG Concentration (mM)	Induction Time (hours)	Fusion Protein Yield*	
		30 °C	37 °C
0.05	0	0.91 ± 0.04	0.86 ± 0.02
	0.5	0.89 ± 0.02	0.99 ± 0.02
	1	1.07 ± 0.04	1.08 ± 0.01
	2	1.60 ± 0.01	1.83 ± 0.01
	3	1.44 ± 0.04	1.29 ± 0.11
	4	1.34 ± 0.03	1.91 ± 0.01
1	0	0.91 ± 0.06	0.87 ± 0.01
	0.5	0.82 ± 0.01	0.99 ± 0.04
	1	0.98 ± 0.03	1.08 ± 0.03
	2	1.38 ± 0.09	1.90 ± 0.08
	3	1.36 ± 0.02	2.21 ± 0.07
	4	1.31 ± 0.01	2.16 ± 0.09

\*Ratio of protein concentration with IPTG induction divided by protein concentration with no IPTG induction (endogeneous bacterial protein synthesis). Mean  $\pm$  s.e.m. of duplicate measurements.

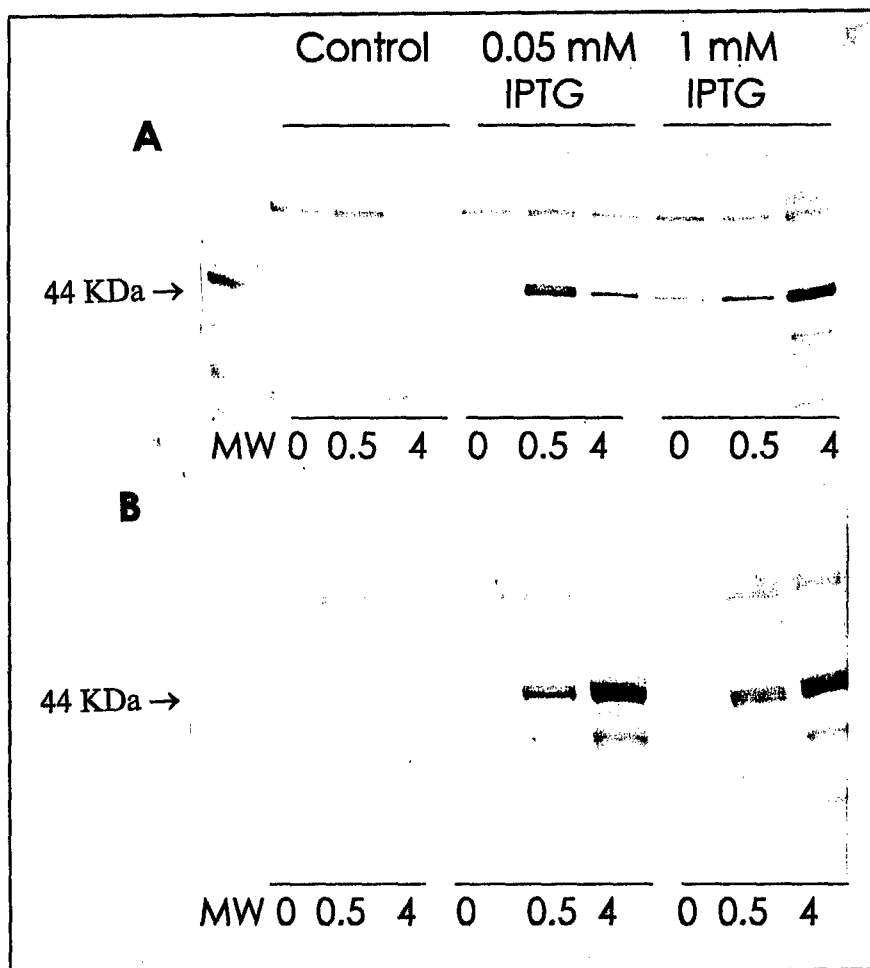


**Fig. 3.** Western blot of bacterial cell lysate using polyclonal anti-EGF antibody at 0, 0.5 and 4 hours of induction with IPTG. **A.** Incubation temperature 30 °C. **B.** Incubation temperature 37 °C. IPTG concentration was 0.05 mM. Lanes marked "control" represent no IPTG induction. Band at  $M_r$  of 44 kDa represents hEGF-C<sub>H</sub>1-GST fusion protein.

### 3. Purification of hEGF-C<sub>H</sub>1 protein under "native" conditions

The majority of the hEGF-C<sub>H</sub>1 fusion protein is present in inclusion bodies in *E. coli* and therefore requires purification using denaturing conditions with 8 M urea or 6 M guanidine, followed by refolding of the protein (see section 5). However, a small amount (approx. 100 mg) of the hEGF-C<sub>H</sub>1 fusion protein was recovered using non-danaturing, "native" conditions (Fig. 4). The hEGF-C<sub>H</sub>1 protein was purified by affinity chromatography on an anti-GST column. The hEGF-C<sub>H</sub>1 protein can also be purified by metal-chelating affinity chromatography on a Ni-agarose column because the C<sub>H</sub>1 gene contains a polyhistidine tail. The purity of the hEGF-C<sub>H</sub>1 protein was then determined by SDS-PAGE and Western blot and its receptor-binding properties were evaluated by flow cytometry and ELISA (see section 4). The SDS-PAGE analysis (Fig. 5) indicated that we obtained a pure protein with the expected  $M_r$  for hEGF-C<sub>H</sub>1 fused to GST (~44 kDa).

The GST domain was subsequently removed by enzymatic cleavage using thrombin. A Western blot of the final enzymatically cleaved hEGF-C<sub>H</sub>1 protein demonstrated a protein with the expected molecular weight ( $M_r$  18 kDa) (Fig. 6).

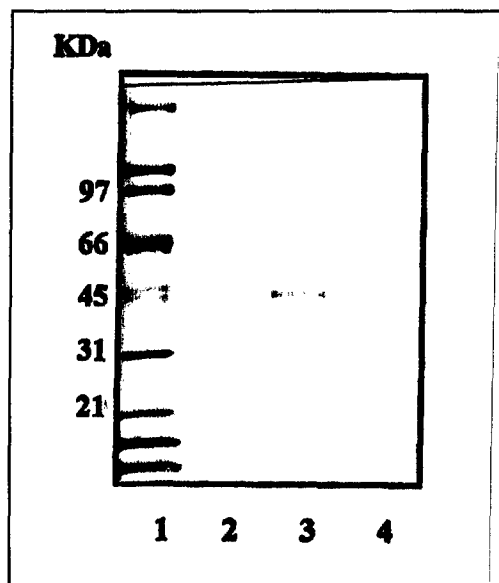


**Fig. 5.** SDS-PAGE analysis of hEGF-C<sub>H</sub>1 protein fused to GST on a 4-20% Tris-HCl mini-gel stained with Coomassie blue R-250. The pure hEGF-C<sub>H</sub>1-GST protein is indicated by the single band in lanes 3 and 4 with a  $M_r$  of 44 kDa. Lane 2 represents expression without IPTG.

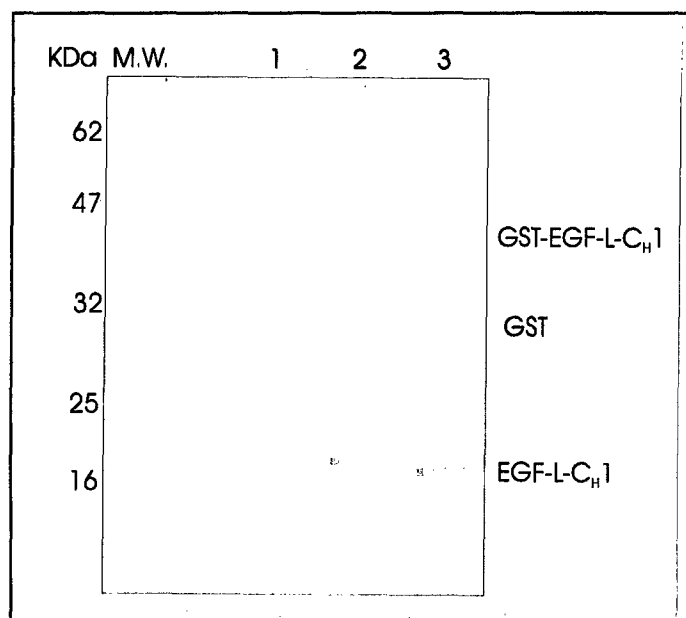


**Fig. 6.** Western blot of final hEGF-C<sub>H</sub>1 fusion protein using an anti-EGF polyclonal antibody showing a single band with the expected molecular weight ( $M_r$  18 kDa).

#### 4. Evaluation of receptor binding properties

The receptor-binding properties of the hEGF-C<sub>H</sub>1-GST fusion protein were evaluated by 1) flow cytometry against MDA-MB-468 human breast cancer cells

and 2) by ELISA against EGFR purified from MDA-MB-468 cells. Flow cytometry demonstrated that the hEGF-C<sub>H</sub>1 fusion protein retained its receptor-binding properties when compared to hEGF (Fig. 4), but the binding was higher when the flexible peptide linker was present, probably due to less steric hindrance in the binding of the hEGF domain from the C<sub>H</sub>1 domain.

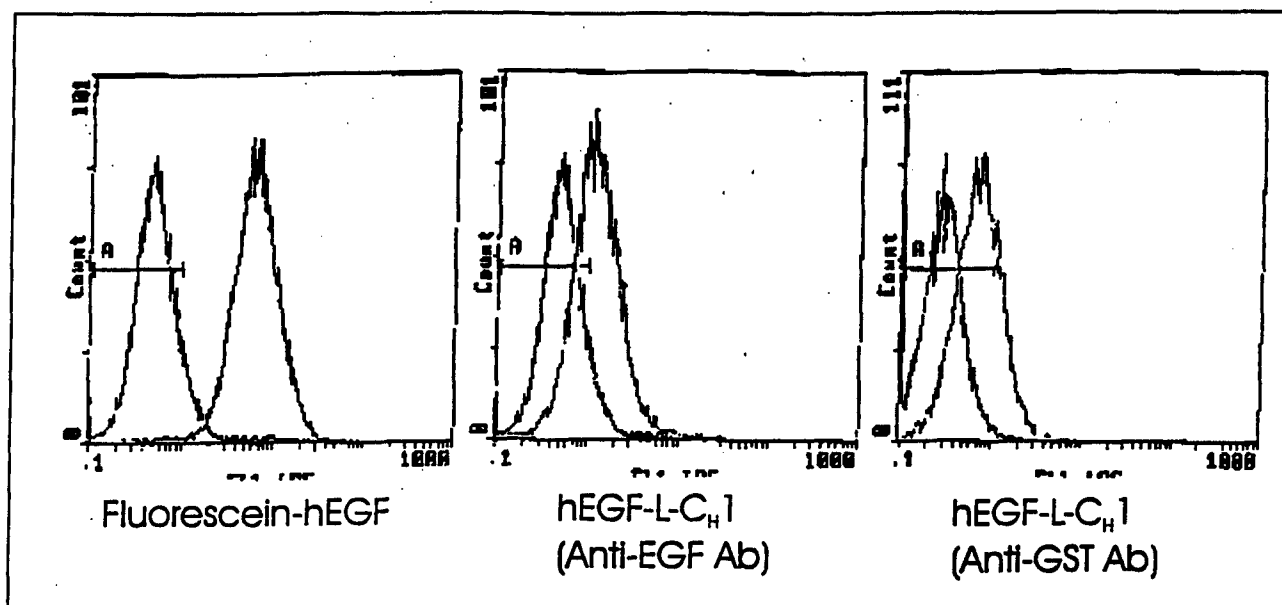


**Fig. 7.** Analysis of the receptor-binding properties of hEGF and hEGF-L-C<sub>H</sub>1-GST fusion protein by flow cytometry against MDA-MB-468 human breast cancer cells. The hEGF or hEGF-C<sub>H</sub>1-GST fusion protein was incubated with the cells for 1 hour at 4 °C. The binding of hEGF to the cells was measured using fluorescein-hEGF (left panel). Binding of hEGF-L-C<sub>H</sub>1 to the cells was measured using an anti-EGF (center panel) or anti-GST secondary antibody (right panel) conjugated to fluorescein. A shift to higher fluorescence (right curve in each panel) relative to the PBS control (left curve in each panel) was observed for hEGF and the hEGF-C<sub>H</sub>1 fusion protein. "L" signifies flexible peptide linker.

By ELISA, the hEGF-C<sub>H</sub>1 fusion protein demonstrated higher binding than hEGF, possibly due to greater avidity for soluble EGFR coated on the micro-ELISA plate (Fig. 5). The hEGF-C<sub>H</sub>1 fusion protein may dimerize through the C<sub>H</sub>1 domains, increasing its avidity for the EGFR.

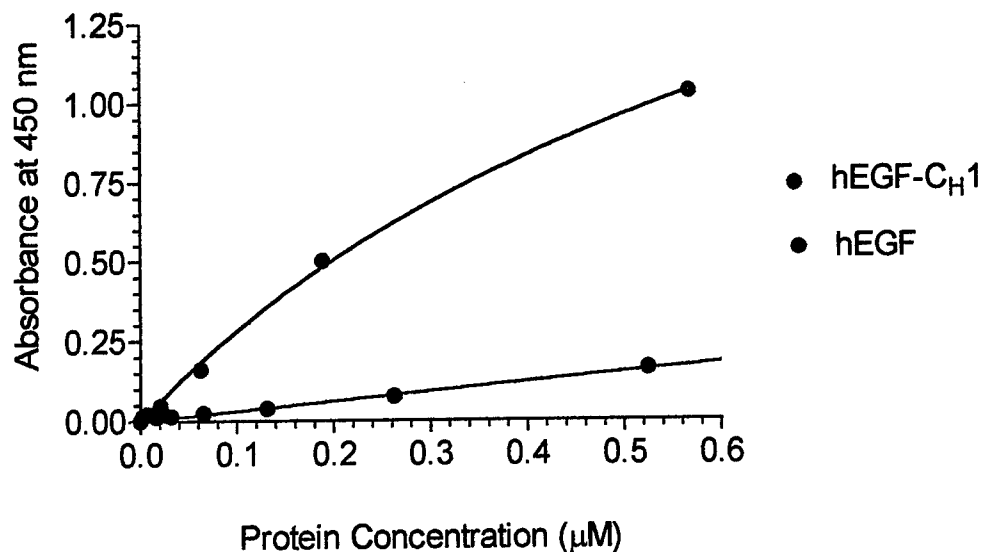


**Fig. 8.** Binding of the hEGF-C<sub>H</sub>1 fusion protein and hEGF to EGFR coated on a microELISA plate. The binding of hEGF-C<sub>H</sub>1 or hEGF was determined using a rabbit polyclonal anti-EGF antibody, anti-rabbit-IgG-HRP and 3,3',5,5'-tetramethylbenzidine (TMB) chromogenic substrate. The absorbance measured in a plate reader at 450 nm.

### 5. Purification of the hEGF-C<sub>H</sub>1 fusion protein using denaturing conditions

As previously described in section 3, the majority of the hEGF-C<sub>H</sub>1 fusion protein is contained in inclusion bodies in *E. coli*. The fusion protein was isolated from inclusion bodies under denaturing conditions and refolded following the method of D'Alatri et al. (5). Briefly, the cells were lysed by ultrasonication, centrifuged and the inclusion bodies were solubilized in a buffer containing 6 M guanidine-HCl and 5 mM imidazole. The denatured hEGF-C<sub>H</sub>1 protein was then purified on a Ni-agarose affinity column eluted with a 50 mM Tris-HCl/6 M guanidine-HCl buffer. The purified, denatured fusion protein was treated with 160 mM dithiothreitol (DTT) for 3 hours at 22 °C and refolded by 100-fold rapid dilution into 50 mM Tris-HCl pH 8.5 containing 0.5 M arginine, 4 mM oxidized glutathione and 2 mM DTT. After incubation for 60 hours at 10°C, the refolded hEGF-C<sub>H</sub>1 protein was concentrated on a Centricon-30 ultrafiltration device. We recovered a small amount of correctly folded hEGF-C<sub>H</sub>1 protein by this method, as indicated by its reactivity with MDA-MB-468 cells by flow cytometry (results not shown). However, the protein precipitated when attempts were made to concentrate it. We believe that the precipitation problem is due to incorrect folding of disulfide bonds which may result in exposure of hydrophobic residues. Work is continuing to investigate alternative procedures for refolding the hEGF-C<sub>H</sub>1 protein. If the problem of refolding cannot be solved in a reasonable time

frame, we will utilize instead properly folded hEGF-C<sub>H</sub>1 protein isolated under native conditions despite the lower yield (see section 3).

## 6. Future work

In the next 3-6 months we expect to be able to purify sufficient quantities of the hEGF-C<sub>H</sub>1 fusion protein for radiolabelling to high specific activity with <sup>111</sup>In and testing for internalization and nuclear translocation in MDA-MB-468 breast cancer cells *in vitro*. Biodistribution studies with the radiolabelled hEGF-C<sub>H</sub>1 fusion protein in athymic mice bearing subcutaneous MDA-MB-468 human breast cancer xenografts are currently in progress and we expect these will also be completed within this time frame. In the next year, clonogenic and colorimetric cell viability assays of MDA-MB-468 breast cancer cells treated with the <sup>111</sup>In-hEGF-C<sub>H</sub>1 fusion protein *in vitro* and evaluation of the <sup>111</sup>In-hEGF-C<sub>H</sub>1 fusion protein for treatment of MDA-MB-468 xenografts in athymic mice will be conducted. In the final year, the efficacy and toxicity of treatment of mice with MDA-MB-468 xenografts with multiple doses of the <sup>111</sup>In-hEGF-C<sub>H</sub>1 fusion protein will be evaluated. Studies combining the <sup>111</sup>In-hEGF-C<sub>H</sub>1 fusion protein and <sup>125</sup>I-labelled estradiol will also be performed.

## KEY RESEARCH ACCOMPLISHMENTS

- Constructed recombinant hEGF-C<sub>H</sub>1 expression vector.
- Optimized conditions for expression of hEGF-C<sub>H</sub>1 fusion protein in E. coli.
- Purified hEGF-C<sub>H</sub>1 fusion protein to homogeneity.
- Tested receptor-binding of hEGF-C<sub>H</sub>1 protein against human breast cancer cells.
- Biodistribution studies of radiolabelled hEGF-C<sub>H</sub>1 in athymic mice with MDA-MB-468 breast cancer xenografts are currently in progress.

## REPORTABLE OUTCOMES

### Manuscripts and Abstracts

*The following manuscripts and abstracts have originated from research funded by our grant from the U.S. Army Breast Cancer Research Program and are included in the Appendices.*

1. Reilly RM, Kiarash R, Cameron R, Porlier N, Sandhu, J., Vallis K., Hendler A, Hill, R.P. and Gariépy J. Indium-111 labelled epidermal growth factor is selectively radiotoxic to human breast cancer cells overexpressing the epidermal growth factor receptor. J. Nucl. Med. (in press) 1999.
2. Reilly R.M., Kiarash R., Sandhu J., Lee YW, Cameron R., Hendler A, Vallis K., and Gariépy J. A comparison of epidermal growth factor and monoclonal antibody 528 labelled with indium-111 for imaging human breast cancer. J. Nucl. Med. (submitted) 1999.
3. Wang J., Sandhu, J., Chen Z., Leung C., Bray M., Yang M., Cameron R., Hendler A., Vallis K., Reilly R.M. Production of a human epidermal growth factor (hEGF)-immunoglobulin (C<sub>H</sub>1) fusion protein for targeting human breast cancer. J. Nucl. Med. 40: 312P, 1999.

#### Presentations

1. Reilly RM. The Trojan Horse: Targeted Auger Electron Radiotherapy of Breast Cancer. Presented at Department of Radiation Oncology Rounds, University of Toronto, February 25, 1999.

#### Patents Applied

Reilly R.M. Radiolabelled peptide ligand for Auger electron radiotherapy of cancer. (U.S. Patent Office-patent pending 1996-Application No. 081/759,282).

#### Other Funding Applied For Based on Work Supported

*The support of the U.S. Army Breast Cancer Program allowed us to discover that peptide growth factors conjugated to Auger electron-emitting radionuclides are potential novel radiotherapeutic agents for cancer. We have proposed the following research proposal to the Natural Sciences and Engineering Research Council of Canada to extend this strategy to the treatment of gliomas using a VEGF fusion protein conjugated with <sup>111</sup>In.*

Natural Sciences and Engineering Research Council of Canada. 1999-2001. Vascular growth factor receptors as a target for Auger electron radiotherapy of malignant astrocytomas. J. Sandhu, R.M. Reilly (co-investigator) and A. Guha. \$ 252,000 applied.

#### CONCLUSIONS

A recombinant hEGF-C<sub>H</sub>1 fusion protein was produced in E. coli for targeting human breast cancer with the Auger electron-emitting radionuclide, <sup>111</sup>In. The hEGF-C<sub>H</sub>1 protein binds to MDA-MB-468 human breast cancer cells *in vitro* by

flow cytometry and to EGFR by ELISA. Animal studies are in progress to evaluate the ability of the fusion protein to target MDA-MB-468 human breast cancer xenografts *in vivo*. This novel hEGF-C<sub>H</sub>1 fusion protein is a potential targeting vehicle for delivering radionuclides to EGFR-positive cancer cells for diagnostic imaging and/or radiotherapy of the disease.

## **REFERENCES**

1. Klijn JGM, Berns PMJ, Schmitz PIM, Foekens JA. The clinical significance of epidermal growth factor receptor (EGF-R) in human breast cancer: a review on 5232 patients. Endocr. Rev. 13: 3-17, 1992
2. Reilly RM, Kiarash R, Cameron R, Porlier N, Sandhu J, Vallis K, Hendler A, Hill RP and Gariépy J. Indium-111 labelled epidermal growth factor is selectively radiotoxic to human breast cancer cells overexpressing the epidermal growth factor receptor. J. Nucl. Med. (in press) 1999.
3. Reilly RM, Kiarash R, Sandhu J, Lee YW, Cameron R, Hendler A, Vallis K, and Gariépy J. A comparison of epidermal growth factor and monoclonal antibody 528 labelled with indium-111 for imaging human breast cancer. J. Nucl. Med. (submitted) 1999.
4. Wang J, Sandhu, J, Chen Z, Leung C, Bray M, Yang M, Cameron R, Hendler A, Vallis K and Reilly RM Production of a human epidermal growth factor (hEGF)-immunoglobulin (C<sub>H</sub>1) fusion protein for targeting human breast cancer. J. Nucl. Med. 40: 312P, 1999.
5. D'Alatri L, Di Massimo AM, Anastasi AM et al. Production and characterization of a recombinant single-chain anti ErbB2-clavin immunotoxin. Anticancer Res. 18: 3369-3374, 1998.

## **APPENDICES**

## **Indium-111 Labelled Epidermal Growth Factor is Selectively Radiotoxic to Human Breast Cancer Cells Overexpressing the Epidermal Growth Factor Receptor**

Raymond M. Reilly, Ph.D., Reza Kiarash, B.Sc., Ross G. Cameron, M.D., Ph.D, Nicole Porlier, B.Sc., Jasbir Sandhu, Ph.D, Richard P. Hill, Ph.D., Katherine Vallis, M.D., Ph.D., Aaron Hendler, M.D. and Jean Gariépy, Ph.D.

*Division of Nuclear Medicine (R.M.R., R.K., N.P., A.H.) and Department of Pathology (R.G.C.) Toronto General Hospital and Department of Radiation Oncology (K.V.), Princess Margaret Hospital, University Health Network; Samuel Lunenfeld Research Institute, Mount Sinai Hospital (J.S.); Departments of Medical Imaging (R.M.R., A.H.), Pharmaceutical Sciences (R.M.R.) and Medical Biophysics (R.P.H., J.G.) University of Toronto.*

Address correspondence and requests for reprints to:

Raymond M. Reilly and Jean Gariépy  
Division of Nuclear Medicine, Toronto General Hospital  
University Health Network  
585 University Ave.  
Toronto, ON, Canada  
M5G 2C4  
Tel.: (416) 340-3036  
FAX: (416) 340-5065  
e-mail: raymond.reilly@utoronto.ca

Revised: May 21, 1999

This research was supported in part by grants from DuPont Pharma, the Susan G. Komen Breast Cancer Foundation (Grant No. 9749) and the U.S. Army Breast Cancer Research Program (Grant No. DAMD17-98-1-8171) to R.M.R. and a grant from the National Cancer Institute of Canada with funds from the Canadian Cancer Society to J.G. Parts of this study were presented at the Canadian Association of Nuclear Medicine Meeting, Ottawa, ON, Canada, November 10, 1997.

Running Footline: Radiotoxicity of In-111 EGF Against Breast Cancer

**ABSTRACT**

Our objective was to determine if the internalization and nuclear translocation of human epidermal growth factor (hEGF) following binding to its cell surface receptor (EGFR) could be exploited to deliver the Auger electron emitter,  $^{111}\text{In}$  into EGFR-positive breast cancer cells for targeted radiotherapy. **Methods:** hEGF was derivatized with diethylenetriaminepentaacetic acid (DTPA) and radiolabelled with  $^{111}\text{In}$  acetate. The internalization of  $^{111}\text{In}$ -DTPA-hEGF by MDA-MB-468 breast cancer cells ( $1.3 \times 10^6$  EGFR/cell) was determined by displacement of surface-bound radioactivity by an acid-wash. The radioactivity in the cell nucleus and chromatin, isolated by differential centrifugation was measured. The effect on the growth rate of MDA-MB-468 or MCF-7 ( $1.5 \times 10^4$  EGFR/cell) cells was determined following treatment *in vitro* with  $^{111}\text{In}$ -DTPA-hEGF, unlabelled DTPA-hEGF or  $^{111}\text{In}$ -DTPA. The surviving fraction of MDA-MB-468 or MCF-7 cells treated *in vitro* with  $^{111}\text{In}$ -DTPA-hEGF was determined in a clonogenic assay. The radiotoxicity *in vivo* against normal hepatocytes or renal tubular cells was evaluated by measuring alanine aminotransferase (ALT) or creatinine levels in mice administered high amounts of  $^{111}\text{In}$ -DTPA-hEGF (equivalent to human doses up to 14,208 MBq) and by light and electron microscopy of the tissues. **Results:** Approximately 70% of  $^{111}\text{In}$ -DTPA-hEGF was internalized by MDA-MB-468 cells within 15 minutes at 37 °C and up to 15% was translocated to the nucleus within 24 hours. Chromatin contained 10% of internalized radioactivity. The growth rate of MDA-MB-468 cells was decreased 3-fold by treatment with  $^{111}\text{In}$ -DTPA-hEGF (45-60 mBq/cell). Treatment with unlabelled DTPA-hEGF caused a 1.5-fold decrease in growth rate while treatment with  $^{111}\text{In}$ -DTPA had no effect. Targeting of MDA-MB-468 cells with up to 130 mBq/cell of  $^{111}\text{In}$ -DTPA-hEGF resulted in a 2-log decrease in their surviving fraction. There was no decrease in the growth rate or surviving fraction of MCF-7 cells. There was no evidence of hepatotoxicity or renal toxicity in mice administered high amounts of  $^{111}\text{In}$ -DTPA-hEGF. Radiation dosimetry estimates suggest that the radiation dose to a MDA-MB-468 cell targeted with  $^{111}\text{In}$ -DTPA-hEGF could be as high as 25 Gy with up to 19 Gy delivered to the cell nucleus. **Conclusion:**  $^{111}\text{In}$ -DTPA-hEGF is a promising novel radiopharmaceutical for targeted Auger electron radiotherapy of advanced, hormone-resistant breast cancer.

**Key words:** breast cancer; epidermal growth factor; indium-111, Auger electrons; epidermal growth factor receptor

## INTRODUCTION

Over the past decade, numerous studies have investigated the potential for targeted radiotherapy of human malignancies using monoclonal antibodies (mAbs) directed against tumour-associated antigens conjugated with  $\beta$ -particle emitting radionuclides (radioimmunotherapy) (reviewed in (1)). Although promising results have been achieved in B-cell lymphomas, radioimmunotherapy has generally been ineffective for the treatment of solid tumours due to dose-limiting bone marrow toxicity. Non-specific myelotoxicity was due to high levels of circulating radioactive antibodies perfusing the bone marrow combined with the long path length (2-10 mm) of the  $\beta$ -particles. Auger electron emitting radionuclides, such as  $^{125}\text{I}$  and  $^{111}\text{In}$  represent an appealing alternative to  $\beta$ -particle emitters for targeted radiotherapy of cancer (2). Most Auger electrons have an energy of <30 keV and a very short, subcellular path length in tissues (2-12 nm). Thus, Auger electron emitters can only exert their radiotoxic effects on cells when internalized into the cytoplasm and particularly when they are imported into the cell nucleus (3). The high doses of radiation delivered to the cell nucleus from internalized Auger electron-emitting radionuclides are able to cause DNA fragmentation and cell death (4). Decay of an Auger electron emitting radionuclide outside the cell or at the cell surface delivers an insufficient dose of radiation to cause radiotoxicity (5). The selective toxicity of Auger electron emitters towards cells which can bind and internalize the radionuclide could, in theory, minimize or even eliminate the non-specific radiotoxicity against bone marrow stem cells which was previously observed with the use of  $\beta$ -emitters in radioimmunotherapy.

Iodine-125 iododeoxyuridine ( $^{125}\text{I}$ -UdR), one of the most widely studied Auger electron-emitting radiopharmaceuticals is a radiolabelled thymidine analog which is transported into cells and incorporated directly into DNA during S-phase (6).  $^{125}\text{I}$ -UdR is highly radiotoxic to mammalian cells (7) but has limitations as a radiotherapeutic agent due to its relative lack of specificity for tumour cells, targeting of cells only in S-phase and its extensive deiodination in the liver. Nevertheless,  $^{125}\text{I}$ -UdR is currently being investigated for the treatment of bladder cancer (8), gliomas (9) and hepatic metastases (10) where normal tissue uptake can be minimized by local administration.

The Auger electron emitter,  $^{111}\text{In}$ , is also radiotoxic to cells when internalized (11). For example,  $^{111}\text{In}$ -oxine, a lipophilic chelate which diffuses non-specifically into cells used for radiolabelling leukocytes for imaging of infection, can cause DNA damage to lymphocytes (eg. gaps, breaks and exchanges in chromosomes) and is potentially radiotoxic and mutagenic to the cells (12).  $^{111}\text{In}$ -oxine is also radiotoxic to hematopoietic stem cells (11), fibroblasts (5) and cervical carcinoma cells (13).  $^{111}\text{In}$ -oxine is not suitable as a radiotherapeutic agent because it internalizes non-specifically into both normal and malignant cells, but these observations suggest that  $^{111}\text{In}$  could be a very effective Auger electron emitter for radiotherapy of cancer, if the radionuclide could be specifically targeted and internalized into malignant cells.

One possible strategy for selectively delivering  $^{111}\text{In}$  into cancer cells would be to exploit the normal internalization pathway for peptide growth factors following their binding to cell surface receptors. This pathway involves internalization of growth factors and their receptors into cytoplasmic vesicles for proteolytic degradation and in some cases, may also include nuclear translocation (14). Receptors for peptide growth factors are expressed at much higher levels in certain types of malignancies (15) than on normal cells and are therefore potential targets for radiopharmaceuticals. For instance, octreotide is an octapeptide analog of somatostatin which has been radiolabelled with  $^{111}\text{In}$  ( $^{111}\text{In}$ -pentetreotide) and used successfully to image tumours which overexpress somatostatin receptors (16). The internalization of  $^{111}\text{In}$ -pentetreotide and its translocation to the cell nucleus after binding to the somatostatin receptor (17), also makes the radiopharmaceutical a promising candidate for targeted Auger electron radiotherapy of somatostatin receptor-positive tumours (18).

Overexpression of the epidermal growth factor receptor (EGFR) at levels up to 100 times higher than that observed on normal epithelial cells has been observed in 30-60% of human breast cancer biopsies (reviewed in (19)). EGFR overexpression is an attractive target for the design of novel therapies for breast cancer because it is present in almost all estrogen receptor-negative and hormone-resistant, advanced forms of the disease and is also associated with a poor prognosis (19). Such patients are candidates for systemic chemotherapy but response rates to current regimens are inadequate and long term survival is poor (20). There is an urgent need to develop alternate treatment strategies. Our objective was to investigate the internalization, nuclear translocation and radiotoxicity of human epidermal growth factor (hEGF) radiolabelled with the Auger electron emitter  $^{111}\text{In}$ , against EGFR-positive human breast cancer cells, as well as the radiotoxicity of the radiopharmaceutical against normal tissues known to express moderate to high levels of the receptor. Our findings suggest that the application of targeted Auger electron radiotherapy using  $^{111}\text{In}$ -hEGF for the treatment of hormone-resistant forms of breast cancer which overexpress the EGFR may be a promising therapeutic strategy.

## **MATERIALS AND METHODS**

### **Breast cancer cells**

The human breast cancer cell line MDA-MB-468 was purchased from the American Type Culture Collection (Rockville, MD) and the MCF-7 human breast cancer cell line was obtained from Dr. A. Marks at the Banting and Best Department of Medical Research, University of Toronto. MDA-MB-468 cells were cultured in L-15 medium (Sigma, St. Louis, MO) supplemented with 10% fetal calf serum (FCS) and MCF-7 cells were maintained in Minimal Essential Medium (Sigma, St. Louis, MO) supplemented with 10% FCS, non-essential amino acids and glutamine (Gibco, Life Technologies, Burlington, ON).

### **Radiolabelling of hEGF and measurement of receptor binding *in vitro***

hEGF (Upstate Biotechnology, Lake Placid, NY) was derivatized with DTPA and radiolabelled with  $^{111}\text{In}$  to a specific activity of 3.7-11.1 MBq/mg (22,200-66,600 MBq/mmol) as previously described (21). The radiochemical purity of  $^{111}\text{In}$ -DTPA-hEGF as assessed by silica gel instant thin layer chromatography in 100 mM sodium citrate pH 5 was 95-98%.  $^{111}\text{In}$ -DTPA-hEGF bound specifically to its receptor on MDA-MB-468 or MCF-7 human breast cancer cells with an affinity constant ( $K_a$ ) of  $7.5 \times 10^8 \text{ L/mol}$  or  $3.9 \times 10^9 \text{ L/mol}$  respectively. The number of receptors/cell ( $B_{\text{max}}$ ) for  $^{111}\text{In}$ -DTPA-hEGF on MDA-MB-468 cells was calculated to be  $1.3 \pm 0.7 \times 10^6$  while  $1.5 \pm 0.7 \times 10^4$  receptors/cell were present on MCF-7 cells.

### **Fluorescence microscopy of breast cancer cells**

hEGF was derivatized with fluorescein isothiocyanate as previously described by Haigler et al. (14) and purified from excess fluorescein by size-exclusion chromatography on a P-2 (BioRad, Mississauga, ON) mini-column eluted with 150 mM sodium chloride. The intracellular localization of hEGF in MDA-MB-468 human breast cancer cells was evaluated by fluorescence microscopy using fluorescein-hEGF and the fluorescent nuclear stain, 4'6'-diamidino-2-phenylindole dihydrochloride (DAPI, Boehringer-Mannheim, Laval, PQ, Canada). Briefly,  $3 \times 10^4$  MDA-MB-468 cells were seeded onto chamber slides (Nunc, Life Technologies, Burlington, ON, Canada) and cultured for 48 hours. The adherent cells were washed 3 times with 150 mM sodium chloride and the slides were incubated in 100 nM fluorescein-hEGF for 1 hour at 37 °C. The fluorescein-hEGF solution was then removed and the slides were washed 3 times with 150 mM sodium chloride. The slides were then incubated with 100 mM DAPI for 10 minutes at 37 °C and again washed 3 times with 150 mM sodium chloride. The slides were fixed in 0.8% glutaraldehyde (Sigma, St. Louis, MO) and examined with a fluorescence microscope to view the localization of the DAPI ( $I_{\text{excit}}$  340-380 nm) and fluorescein ( $I_{\text{excit}}$  470-490 nm) probes.

### **Intracellular localization of $^{111}\text{In}$ -DTPA-hEGF in breast cancer cells**

The intracellular localization of  $^{111}\text{In}$ -DTPA-hEGF was determined by incubating the radiopharmaceutical (5 ng) with  $3 \times 10^6$  MDA-MB-468 cells in 1 mL of 0.1% w/v human serum albumin in 150 mM sodium chloride in 35 mm culture dishes. Using this amount of  $^{111}\text{In}$ -DTPA-hEGF, approximately 12% of EGF receptors were bound by the radiopharmaceutical. The dishes were incubated for 0.25, 0.5, 1, 2, 3, 4 or 24 hours at 37 °C. The proportion of  $^{111}\text{In}$  radioactivity bound to cells at the selected times was determined by transferring cell suspensions to tubes and separating the cell pellet from the supernatant by centrifugation ( $8,600 \times g$  for 5 minutes). Each fraction was then counted in a g-scintillation counter (Auto Gamma model 5650, Packard Instruments, Downer's Grove, IL). The proportion of  $^{111}\text{In}$  radioactivity internalized by cells was determined as previously described for  $^{125}\text{I}$ -EGF by Olsson and co-workers (22) by re-suspending and incubating the cell pellet in 1 mL of 200 mM sodium

acetate/500 mM sodium chloride pH 2.5 at 4 °C for 5 minutes. The tubes were then centrifuged again to separate the internalized  $^{111}\text{In}$  radioactivity (cell pellet) from the non-internalized  $^{111}\text{In}$  radioactivity (supernatant).

Nuclear binding of  $^{111}\text{In}$ -DTPA-hEGF in MDA-MB-468 human breast cancer cells was determined as previously described for  $^{125}\text{I}$ -EGF (23). The MDA-MB-468 cells were first incubated with  $^{111}\text{In}$ -DTPA-hEGF, then the treated cells were transferred to tubes and centrifuged at 600 x g for 10 minutes to recover the cell pellet. The pellet was then resuspended in a buffer containing 350 mM sucrose/10 mM KCl/1.5 mM  $\text{MgCl}_2$ /10 mM Tris hydrochloride pH 7.6 with 0.2% Triton X-100 (BioRad, Mississauga, ON, Canada) and 12 mM 2-mercaptoethanol and the cells were disrupted by sonication for 5 minutes in an ultrasonic bath. Cell nuclei were isolated by centrifugation of the cell suspension at 900 x g for 10 minutes. Chromatin was isolated from the nuclei by first washing the nuclear pellet with a buffer containing 200 mM sucrose/3 mM calcium chloride/50 mM Tris hydrochloride pH 7.6, followed by a wash step in 140 mM sodium chloride/10 mM Tris hydrochloride pH 8.3 and finally by pelleting the suspension at 900 x g for 10 minutes. The supernatant containing the nucleoplasmic proteins was discarded. The nuclei were then swollen in a small amount of 1 mM Tris hydrochloride pH 7.9 and centrifuged at 1,700 x g for 10 minutes to separate the chromatin fraction from the supernatant which contained the nucleoplasm and nuclear membranes.

#### **Growth inhibition of human breast cancer cells *in vitro* by $^{111}\text{In}$ -DTPA-hEGF**

The effect of treating MDA-MB-468 or MCF-7 cells *in vitro* with  $^{111}\text{In}$ -DTPA-hEGF on their growth was determined by incubating  $2 \times 10^7$  breast cancer cells in 1 mL of 150 mM sodium chloride in a sterile 35 mm culture dish in the presence of an excess of  $^{111}\text{In}$ -DTPA-hEGF (5 mg, 11.1 MBq) at 37 °C for 30 minutes. The amount of  $^{111}\text{In}$ -DTPA-hEGF added represented a 25-fold excess for MDA-MB-468 cells and a 2,500-fold excess for MCF-7 cells. The cells were then transferred to a sterile polystyrene culture tube and centrifuged at 600 x g for 5 minutes. The amount of  $^{111}\text{In}$  radioactivity associated with the cell pellet was measured in a radioisotope calibrator (Model CRC-12, Capintec, Montvale, NJ) and divided by the number of treated cells to calculate the average amount of  $^{111}\text{In}$  radioactivity targeted to each cell (milli-Becquerel/cell [mBq/cell]). The cells were then resuspended in growth medium and  $5 \times 10^5$  cells were seeded into six replicate 60 mm culture dishes. The cells were cultured for a period of 7 days. Control dishes contained untreated cells, cells treated with unlabelled DTPA-hEGF (5 mg) or cells incubated with growth medium containing a concentration of  $^{111}\text{In}$ -DTPA (11 kBq/mL, DraxImage, Dorval, PQ, Canada) equivalent to the amount of  $^{111}\text{In}$ -DTPA-hEGF bound to the treated cells. At day 1 and day 7, cells were recovered from dishes using trypsin/EDTA and counted in a hemocytometer. The growth index was defined as the number of cells recovered at day 7 divided by the number of cells recovered at day 1. The average number of cells recovered at the two time points and the average growth index was determined and compared for treated and untreated cells. Both the treated and

control dishes contained cells which were sub-confluent throughout the 7-day experiment.

### **Radiotoxicity of $^{111}\text{In}$ -DTPA-hEGF against human breast cancer cells *in vitro***

The radiotoxicity of  $^{111}\text{In}$ -DTPA-hEGF against MDA-MB-468 or MCF-7 human breast cancer cells was determined in a clonogenic assay. Increasing amounts of  $^{111}\text{In}$ -DTPA-hEGF (37 kBq-2.6 MBq, 0.01-70 mg) were dispensed into sterile 35 mm culture dishes containing  $5 \times 10^5$  MDA-MB-468 or MCF-7 cells in 1 mL of 150 mM sodium chloride. The maximum amounts of  $^{111}\text{In}$ -DTPA-hEGF added represented a 1,400-fold molar excess for MDA-MB-468 cells and a 140,000-fold molar excess for MCF-7 cells. The dishes were incubated for 30 minutes at 37 °C then the cells were recovered and assayed for the average amount of  $^{111}\text{In}$  radioactivity targeted to each cell (mBq/cell). Sufficient cells ( $3 \times 10^4$  to  $10^6$ ) were then seeded in triplicate into 60 mm sterile culture dishes (Nunc, Life Technologies, Burlington, ON) to obtain a measureable number of colonies after culturing for a period of 10 days at 37 °C. Control dishes contained cells incubated with growth medium alone. At the end of the culture period, the colonies were stained with methylene blue (1% in a 1:1 mixture of ethanol and water) and the number of colonies (>50 cells/colony) in each dish was counted. The plating efficiency was calculated by dividing the number of colonies observed in each dish by the number of cells seeded. The surviving fraction was calculated by dividing the plating efficiency for the dishes containing treated cells by the plating efficiency for the control dishes.

The survival curves for the treated MDA-MB-468 or MCF-7 breast cancer cells were obtained by plotting the log of the mean surviving fraction for the triplicate dishes versus the amount of  $^{111}\text{In}$  radioactivity targeted to the entire cell, internalized into the cytoplasm or associated with the chromatin fraction (mBq/cell). A straight line was then fitted through each of the survival curves by log-linear regression analysis. The  $D_0$  values were estimated from the terminal slope of the regression lines.

### **Evaluation of the hepatotoxicity and renal toxicity of $^{111}\text{In}$ -DTPA-hEGF**

To evaluate the potential for acute hepatotoxicity and renal toxicity from  $^{111}\text{In}$ -DTPA-hEGF, groups of normal Balb/c mice were injected in the tail vein with 3.7, 9.25, 18.5 or 44 MBq of  $^{111}\text{In}$ -DTPA-hEGF in 100 mL of 150 mM sodium chloride. Control mice received a tail vein injection of 150 mM sodium chloride. Prior to injection of  $^{111}\text{In}$ -DTPA-hEGF and at 24, 48 and 72 hours post-injection, blood samples were obtained by nicking the tail of each mouse with a sterile scalpel blade and collecting 50 mL samples into heparinized capillary tubes (Microcaps, Fisher Scientific Co., Nepean, ON). The blood samples were transferred to microcentrifuge tubes and centrifuged at  $10,600 \times g$  for 5 minutes to separate the plasma. The plasma samples were stored at -10 °C for subsequent measurement of alanine aminotransferase (ALT) concentrations by standard clinical biochemistry techniques. At 72 hours post-injection, the mice

were sacrificed by cervical dislocation and samples of the liver and kidneys were removed, sectioned and examined by light and electron microscopy for morphological evidence of hepatic or renal toxicity.

The potential for hepatotoxicity and renal toxicity of  $^{111}\text{In}$ -DTPA-hEGF over a longer time period was investigated by administering two separate amounts of the radiopharmaceutical to athymic mice (37 and 74 MBq) by tail vein injection separated by an interval of 4 weeks. Blood samples were collected prior to the first administration of the radiopharmaceutical, then every 3-4 days and the plasma was separated and analysed for ALT and creatinine concentrations as previously described. The mice were sacrificed 7 weeks after the first administration of the radiopharmaceutical and the liver and kidneys were removed, sectioned and examined by light and electron microscopy for morphological evidence of hepatic or renal toxicity. Animal studies were conducted under an approved Animal Care Protocol (# 94-036) at the Toronto Hospital and following the Canadian Council on Animal Care (CCAC) guidelines.

## RESULTS

### Fluorescence microscopy of breast cancer cells

Fluorescence microscopy of MDA-MB-468 human breast cancer cells incubated with fluorescein-hEGF showed binding to the cell surface, internalization into cytoplasmic vesicles and localization to the cell nucleus. After 1 hour of incubation with fluorescein-hEGF at 37 °C, a relatively low level of fluorescence was observed diffusely throughout the cytoplasm of the cells with an intense fluorescence signal associated with the cell nucleus (Fig. 1). The cell nucleus was visualized for comparison using the fluorescent nuclear stain, DAPI (Fig. 1).

### Intracellular localization of $^{111}\text{In}$ -DTPA-hEGF in breast cancer cells

$^{111}\text{In}$ -DTPA-hEGF was rapidly bound and internalized by MDA-MB-468 cells *in vitro* at 37 °C (Table 1). The internalized fraction increased from approximately 70% at 15 minutes of incubation to about 80% at 4 hours. After 30 minutes of incubation of  $^{111}\text{In}$ -DTPA-hEGF with cells, a small proportion of  $^{111}\text{In}$  radioactivity (approximately 7%) was localized in the cell nucleus and 2.5% was associated with the chromatin fraction (Table 2). The fraction of radioactivity in the cell nucleus increased to >15% at 24 hours, with almost 10% associated with the chromatin.

### Growth inhibition of human breast cancer cells *in vitro* by $^{111}\text{In}$ -DTPA-hEGF

Treatment of  $2 \times 10^7$  MDA-MB-468 or MCF-7 human breast cancer cells *in vitro* with a 25-fold or 2,500-fold molar excess of  $^{111}\text{In}$ -DTPA-hEGF (5 mg, 11.1 MBq) resulted in targeting of an average of 45-60 mBq of  $^{111}\text{In}$ -DTPA-hEGF to each cell. The majority of the  $^{111}\text{In}$ -DTPA-hEGF targeted to MCF-7 cells was non-specifically bound however, since only a maximum of 3.7 mBq of  $^{111}\text{In}$ -DTPA-hEGF could, in theory, be specifically targeted to these cells at the receptor

saturation conditions employed (specific activity of the radiopharmaceutical, 22,200 MBq/mmol and the level of expression of the EGFR on these cells,  $1.5 \times 10^4$  EGFR/cell). It was assumed that non-specifically bound  $^{111}\text{In}$ -DTPA-hEGF does not undergo receptor-mediated internalization and would not be expected to be radiotoxic.

There was a significant decrease in the growth index of MDA-MB-468 cells treated with  $^{111}\text{In}$ -DTPA-hEGF compared to untreated cells ( $1.3 \pm 0.2$  versus  $3.7 \pm 0.6$  respectively,  $p < 0.0001$ , Table 3). MDA-MB-468 cells treated with unlabelled DTPA-hEGF also exhibited a significantly lower growth index compared to untreated cells but the magnitude of the decrease was smaller ( $2.5 \pm 0.6$  versus  $3.7 \pm 0.6$  respectively,  $p < 0.01$ ). MDA-MB-468 cells are reported to be growth-inhibited by concentrations of EGF  $> 10^{-9}$  M (24). The concentration of unlabelled DTPA-hEGF in the incubation medium for the growth inhibition assay was  $8 \times 10^{-7}$  M (ie. 5 mg in 1 mL). The growth index of MDA-MB-468 cells treated with  $^{111}\text{In}$ -DTPA, a radiopharmaceutical which does not bind to cells and is not internalized non-specifically, was not significantly different from the growth index of untreated cells ( $3.1 \pm 0.1$  versus  $3.7 \pm 0.6$  respectively,  $p = 0.169$ ). There was also no significant change in the growth index of MCF-7 cells, which have a 100-fold lower level of receptors on their surface than MDA-MB-468 cells ( $1.5 \times 10^4$  versus  $1.3 \times 10^6$  EGFR/cell respectively) treated with  $^{111}\text{In}$ -DTPA-hEGF compared to untreated cells ( $1.7 \pm 0.7$  versus  $2.5 \pm 0.5$  respectively,  $p = 0.193$ ).

#### **Radiotoxicity of $^{111}\text{In}$ -DTPA-hEGF against human breast cancer cells *in vitro***

The surviving fraction of MDA-MB-468 human breast cancer cells treated *in vitro* with  $^{111}\text{In}$ -DTPA-hEGF was reduced to  $< 3\%$  when the cells bound 130 mBq/cell of  $^{111}\text{In}$ -DTPA-hEGF (Fig. 2). The  $D_0$  value was approximately 40 mBq/cell for radioactivity targeted to the entire cell but only 4 mBq/cell when the survival curve was adjusted for radioactivity associated with the chromatin. The  $D_0$  value obtained from the survival curve adjusted for radioactivity localized in the cytoplasm was 28 mBq/cell. The amount of  $^{111}\text{In}$  radioactivity internalized into the cytoplasm or associated with the chromatin was estimated as 70% and 10% respectively of the total  $^{111}\text{In}$  radioactivity bound to the cells (Tables 1 and 2). There was no significant decrease in the surviving fraction of MCF-7 cells when up to 133 mBq/cell of  $^{111}\text{In}$ -DTPA-hEGF was targeted to the cells (Fig. 2). A slight growth stimulatory effect was observed at low amounts of  $^{111}\text{In}$ -DTPA-hEGF bound to MCF-7 cells ( $< 20$  mBq/cell).

#### **Evaluation of the hepatotoxicity and renal toxicity of $^{111}\text{In}$ -DTPA-hEGF**

Graphs shown in Fig. 3 depict the concentration of alanine aminotransferase (ALT) present in the plasma of Balb/c mice as a function of doses of  $^{111}\text{In}$ -DTPA-hEGF (3.7-44 MBq) and times post injection. Only at the highest dose of radioactivity administered (44 MBq) was there a slight rise in ALT concentration as compared to pre-administration values. No significant changes

were observed in ALT or plasma creatinine concentration in comparison to pre-treatment values over a 7-week period in athymic mice administered two high amounts of  $^{111}\text{In}$ -DTPA-hEGF (37 and 74 MBq) separated by a 4-week time interval. The plasma ALT concentration in these studies ranged in value from 18-46 U/L for treated mice and from 16-40 U/L for control mice (normal values are <40 U/L in humans). The plasma creatinine concentration ranged from 60-78 mmol/L for treated mice and 60-66 mmol/L for control mice (normal values are <105 mmol/L in humans). Morphological evidence of hepatotoxicity would be manifested by subtle mitochondrial changes or proliferation of the smooth endoplasmic reticulum or lysosomes. Renal toxicity would be defined by the occurrence of renal tubular degeneration. Such morphological changes were not observed on the electron micrographs of the liver or kidneys at either early (3 days) or late (7 weeks) time points (Fig. 4).

## DISCUSSION

This study demonstrates for the first time that hEGF radiolabelled with the Auger electron emitting radionuclide,  $^{111}\text{In}$ , is selectively radiotoxic to human breast cancer cells which overexpress the EGFR.  $^{111}\text{In}$ -DTPA-hEGF was rapidly bound by breast cancer cells, internalized into the cytoplasm and transported to the cell nucleus. We hypothesize that the internalization and nuclear translocation of  $^{111}\text{In}$ -DTPA-hEGF would deliver the radionuclide in proximity to chromosomal DNA where emitted Auger electrons would be lethal to cells. The radiotoxicity of  $^{111}\text{In}$ -DTPA-hEGF *in vitro* resulted in a significant decrease in the growth rate of MDA-MB-468 human breast cancer cells ( $1.3 \times 10^6$  EGFR/cell) at relatively low amounts of radioactivity targeted to these cells (45-60 mBq/cell). Similarly, a two-log decrease in the survival of these cells was observed in a clonogenic assay at higher amounts of radioactivity (111-130 mBq/cell). No radiotoxicity was observed against MCF-7 human breast cancer cells which expressed a 100-fold lower level of EGFR ( $1.5 \times 10^4$  receptors/cell) suggesting that the radiopharmaceutical was selectively radiotoxic to cancer cells which overexpress EGFR. In addition, over a 7-week period, there was no evidence of radiotoxicity to liver or kidneys in mice administered high amounts of  $^{111}\text{In}$ -DTPA-hEGF. Liver and kidneys are tissues which exhibit moderate to high levels of EGFR expression ( $\sim 10^5$  receptors/cell) (25,26). These results are thus promising for the application of targeted Auger electron radiotherapy using  $^{111}\text{In}$ -DTPA-hEGF for the treatment of EGFR-overexpressing breast cancer in humans.

Fluorescence microscopy revealed that fluorescein-hEGF binds rapidly to MDA-MB-468 cells, is internalized to the cytoplasm and is subsequently translocated to form a ring of fluorescence surrounding the cell nucleus. The internalization of EGF/EGFR complexes after binding of EGF to its receptor is well documented (27) and nuclear localization of EGF has been observed by fluorescence microscopy and other techniques in A431 epidermoid carcinoma cells (14), SW948 human colon cancer cells (23), fibroblasts (28) and hepatocytes (29). The proportion of internalized EGF molecules imported to the cell nucleus ranged from 1-10% (30) but this value increases to 14-40% under

growth stimulatory conditions (28,29) or in the presence of lysosomal protease inhibitors (31). It is not known if EGF remains bound to its receptor during the nuclear translocation process but the EGFR contains a putative nuclear localization sequence (RRRHIVRKRTLRR) at residues 645-657 which could mediate its nuclear import (32). Specific EGFR binding sites on chromatin have also been detected (30). The nuclear translocation event of EGF is not currently understood, since EGF is thought to affect gene expression indirectly by activation of the *ras* or phosphatidylinositol intracellular signaling pathways.

$^{111}\text{In}$ -DTPA-hEGF was rapidly bound, internalized and transported to the cell nucleus in MDA-MB-468 breast cancer cells. Interestingly, almost two thirds of the radioactivity in the cell nucleus was directly associated with the chromatin, suggesting that internalized  $^{111}\text{In}$ -DTPA-hEGF (perhaps in association with EGFR) may interact directly with nuclear DNA. Similar results have been previously reported for  $^{125}\text{I}$ -EGF by Rakowicz-Szulcynska and co-workers (23) in SW948 human colorectal carcinoma cells which express the EGFR. After incubation of the SW948 cells with  $^{125}\text{I}$ -EGF for 24 hours at 37 °C, >94% of the internalized radioactivity was localized in the cytoplasm and 6% was present in the cell nucleus. The majority of the  $^{125}\text{I}$  radioactivity localized in the cell nucleus was directly associated with the chromatin fraction.

Since chromosomal DNA represents a sensitive target in the cell for the radiotoxic effects of Auger electrons emitted by  $^{111}\text{In}$ , the cellular distribution of  $^{111}\text{In}$ -DTPA-hEGF, will control the radiation dose delivered to the nucleus and consequently the radiotoxicity of the radiopharmaceutical. Recently published cellular dosimetry models (33,34) of Auger electron emitting radionuclides deposited in mammalian cells have estimated that the energy deposited in the cell nucleus is 2-fold greater when  $^{111}\text{In}$  is localized in the cytoplasm compared to a situation where the radionuclide is localized on the cell membrane. The deposition rate however increases by 20 to 35-fold when the radionuclide is localized in the nucleus itself. The radiation doses to an entire cell and to the cell nucleus were calculated (34) based on the following distribution pattern of  $^{111}\text{In}$ -DTPA-hEGF in MDA-MB-468 breast cancer cells: 20% bound to the cell membrane, 80% internalized into the cytoplasm and 15% localized in the cell nucleus. It was assumed that the cellular distribution of  $^{111}\text{In}$ -DTPA-hEGF under receptor saturation conditions would be similar to that observed (Tables 1 and 2) using conditions under which approximately 12% of the receptors were bound by the radiopharmaceutical. The calculated radiation doses to each MDA-MB-468 cell when targeted to receptor saturation with  $^{111}\text{In}$ -DTPA-hEGF (specific activity of 3.7 MBq/mg) was 24.7 Gy while 19.3 Gy was delivered to the cell nucleus (Table 4). More importantly, although only 15% of the  $^{111}\text{In}$ -DTPA-hEGF was localized in the cell nucleus, this fraction accounted for 80% of the total radiation dose to the cell nucleus. The  $^{111}\text{In}$ -DTPA-hEGF in the cytoplasm was responsible for an additional 18% of the radiation dose to the nucleus while the remaining 20% fraction of radiopharmaceutical remaining bound to the cell membrane accounted for only 3% of the radiation dose delivered to the cell nucleus.

The relative radiotoxicity of  $^{111}\text{In}$ -DTPA-hEGF towards MDA-MB-468 cells could not be further assigned to distinct intracellular compartments since the radiopharmaceutical is distributed into multiple compartments (ie. cell membrane, cytoplasm and nucleus). Nevertheless, by adjusting the survival curves for the proportion of radiopharmaceutical bound to chromatin or present in the cytoplasm, a comparison could be made of the potential differences in radiosensitivity due to the radiopharmaceutical being localized in these compartments. The adjusted survival curves (Fig. 2) showed that there could be a 7 to 10-fold greater radiosensitivity of MDA-MB-468 cells when  $^{111}\text{In}$ -DTPA-hEGF is bound to the chromatin ( $D_0$  value of 4 mBq/cell) as compared to a situation where the radiopharmaceutical is localized in the cytoplasm ( $D_0$  value of 28 mBq/cell) or is evenly distributed in the entire cell ( $D_0$  value of 40 mBq/cell).

Most normal tissues express very low levels of the EGFR ( $<10^4$  receptors/cell) and should not be adversely affected by targeted Auger electron radiotherapy of breast cancer using  $^{111}\text{In}$ -DTPA-hEGF. The radiopharmaceutical might be radiotoxic however to the liver (25) and the kidneys (26) which exhibit moderate to high levels of the EGFR ( $\sim 10^5$  receptors/cell). There was no evidence of radiotoxicity to the liver or kidneys of mice administered high amounts of  $^{111}\text{In}$ -DTPA-hEGF corresponding on a MBq/m<sup>2</sup> basis to human amounts of 740-14,208 MBq (surface area of a 25 g mouse is 0.009 m<sup>2</sup> compared to 1.73 m<sup>2</sup> in a 70 kg human). Indeed, over a 7-week observation period, there were no significant increases in the concentration of ALT or creatinine in the plasma and there were no morphological lesions in these organs as detected by light or electron microscopy. The 7-week observation period should have been sufficient to detect at least early damage to the liver, since Wordsworth et al. (35) showed that increases in serum ALT levels occur within a few days in rats administered high doses of  $^{198}\text{Au}$  colloid (calculated to deliver 30-110 Gy to the liver). Hebard et al. (36) found that hepatic injury following administration of  $^{198}\text{Au}$  colloid to rats occurred in two phases: an early phase occurring within the first 2-12 weeks involving fibrosis and infiltration of inflammatory cells into the liver and a late phase occurring at 16-40 weeks manifested by severe vasculature damage. It is nevertheless possible that very late radiation injury to the liver or kidneys could become evident at time points beyond 7 weeks. It is also possible that more subtle forms of liver radiotoxicity may not be seen until the hepatocytes attempt cell division, a process which could require a long period of time for a normally quiescent tissue such as the liver. The radiotoxicity of  $^{111}\text{In}$ -DTPA-hEGF against bone marrow stem cells was not measured in this study, but myelotoxicity is not anticipated since  $<3\%$  of the bone marrow stem cell population has been found to express the EGFR (37) and the radiopharmaceutical must specifically bind and internalize into the cells in order to exert a radiotoxic effect.

One potential limitation to the clinical application of  $^{111}\text{In}$ -DTPA-hEGF for targeted radiotherapy of breast cancer is its rapid rate of elimination from the blood which results in relatively low tumour localization. Studies in athymic mice bearing subcutaneous MDA-MB-468 human breast cancer xenografts

administered  $^{111}\text{In}$ -DTPA-hEGF demonstrated tumour localization with tumour/blood ratios approximately 12:1 but tumour uptake of the radiopharmaceutical at 72 hours post-injection was only 2-3% injected dose/g (38) (Table 5). We believe that the tumour localization of  $^{111}\text{In}$ -DTPA-hEGF *in vivo* can be improved significantly by prolonging its residence time in the blood, since the accumulation of  $^{111}\text{In}$  labelled anti-EGFR monoclonal antibody 528 (which clears much more slowly from the blood than hEGF) in MDA-MB-468 breast cancer xenografts was 10-fold higher (21% injected dose/g) than that observed for  $^{111}\text{In}$ -DTPA-hEGF. We are currently modifying the properties of the hEGF molecule to increase its specific activity and slow its elimination from the blood to improve tumour localization. In future studies, once the pharmacokinetic properties of the radiopharmaceutical have been optimized, we will evaluate the potential for targeted Auger electron radiotherapy of breast cancer *in vivo* in athymic mice bearing MDA-MB-468 human breast cancer xenografts. Another important issue in the clinical application of  $^{111}\text{In}$ -DTPA-hEGF for the treatment of breast cancer is receptor heterogeneity, since the radiopharmaceutical is only radiotoxic to cells which express the EGFR and are able to specifically internalize the radiopharmaceutical. In order to address this potential problem, it may be necessary to utilize a "cocktail" of Auger electron-emitting radiopharmaceuticals. Since EGFR expression is inversely correlated with the expression of estrogen receptors (19) or somatostatin receptors (39),  $^{111}\text{In}$ -DTPA-hEGF could be combined with  $^{125}\text{I}$ -estradiol (40) or  $^{111}\text{In}$ -pentetate (18) to target a higher proportion of tumour cells in a lesion.

## CONCLUSIONS

We have shown for the first time that  $^{111}\text{In}$ -DTPA-hEGF was selectively radiotoxic *in vitro* to human breast cancer cells which overexpress the EGF receptor.  $^{111}\text{In}$ -DTPA-hEGF was rapidly bound by breast cancer cells, internalized into the cytoplasm and transported to the cell nucleus. We hypothesize that the internalization and nuclear translocation of  $^{111}\text{In}$ -DTPA-hEGF delivered the radionuclide in proximity to chromosomal DNA at which the emitted Auger electrons were lethal to the cells. There was no evidence of radiotoxicity associated with the administration of high amounts of the radiopharmaceutical *in vivo* against normal tissues such as the liver or kidneys which exhibit moderate-high levels of EGFR expression over a 7-week observation period in mice. Issues relating to tumour uptake of  $^{111}\text{In}$ -DTPA-hEGF *in vivo* remain to be addressed, but these results are nevertheless encouraging for the application of  $^{111}\text{In}$ -DTPA-hEGF in humans for targeted Auger electron radiotherapy of advanced, hormone-resistant breast cancer overexpressing the EGF receptor.

## Acknowledgements

This research was supported in part by grants from DuPont Pharma, the Susan G. Komen Breast Cancer Foundation (Grant No. 9749) and the U.S. Army Breast Cancer Research Program (Grant No. DAMD17-98-1-8171) to R.M.R. and a

grant from the National Cancer Institute of Canada with funds from the Canadian Cancer Society to J.G.. Parts of this study were presented at the Canadian Association of Nuclear Medicine Meeting, Ottawa, ON, Canada, November 10, 1997.

## REFERENCES

1. Reilly RM. Radioimmunotherapy of malignancies. *Clin Pharm* 1991;10:359-75.
2. Adelstein SJ. The Auger process: A therapeutic promise. *Am J Radiol* 1993;160:707-13.
3. Hofer KG, Harris CR, Smith MJ. Radiotoxicity of intracellular Ga-67, I-125 and H-3. Nuclear versus cytoplasmic radiation effects in murine L1210 leukemia cells. *Int J Radiat Biol Rel Stud Phys Chem Med* 1975;28:225-41.
4. Martin RF, Bradley TR, Hodgson GS. Cytotoxicity of an  $^{125}\text{I}$ -labeled DNA-binding compound that induces double-stranded DNA breaks. *Cancer Res* 1979;39:3244-7.
5. McLean JR, Blakey DH, Douglas GR, Bayley J. The Auger electron dosimetry of indium-111 in mammalian cells *in vitro*. *Radiat Res* 1989;119:205-18.
6. Kassis AI, Fayad F, Kinsey BM, Sastry KSR, Taube RA, Adelstein SJ. Radiotoxicity of  $^{125}\text{I}$  in mammalian cells. *Radiat Res* 1987;111:305-18.
7. Chan PC, Lisco E, Lisco H, Adelstein SJ. The radiotoxicity of iodine-125 in mammalian cells, II. A comparative study on cell survival and cytogenetic responses to  $^{125}\text{IUdR}$ ,  $^{131}\text{IUdR}$ , and  $^3\text{HTdR}$ . *Radiat Res* 1976;67:332-43.
8. Mariani G, Collechi P, Baldassarri S, et al. Tumor uptake and mitotic activity pattern of 5- $^{125}\text{I}$ iodo-2'-deoxyuridine after intravesical infusion in patients with bladder cancer. *J Nucl Med* 1996;37(Suppl.):16S-8S.
9. Kassis AI, Tumeh SS, Wen PYC, et al. Intratumoral administration of 5- $^{123}\text{I}$ iodo-2'-deoxyuridine in a patient with a brain tumor.. *J Nucl Med* 1996;37(Suppl.):19S-21S.
10. Macapinlac HA, Kemeny N, Daghighian F, et al. Pilot clinical trial of 5- $^{125}\text{I}$ iodo-2'deoxyuridine in the treatment of colorectal cancer metastatic to the liver. *J Nucl Med* 1996;37:25S-8S.
11. Kraal G, Geldorf AA. Radiotoxicity of indium-111. *J Immunol Meth* 1979;31:193-5.

12. Ten Berge RJM, Natarajan AT, Hardeman MR, et al. Labeling with In-111 has detrimental effects on human lymphocytes: concise communication. *J Nucl Med* 1983;24:615-20.
13. Danpure HJ, Osman S, Hesslewood IP. Cell damage associated with [<sup>111</sup>In]oxine labeling of human tumor cell line (HeLa S3). *J Labelled Compd Radiopharm* 1979;16:116-7.
14. Haigler H, Ash JF, Singer SJ, Cohen S. Visualization by fluorescence of the binding and internalization of epidermal growth factor in human carcinoma cells A-431. *Proc Natl Acad Sci USA* 1978;75:3317-21.
15. Mendelsohn J. Growth factor receptors as targets for antitumor therapy with monoclonal antibodies. In: Mendelsohn J and Waldmann H, eds. *Monoclonal Antibody Therapy*. Basel: Karger; 1988: 147-60.
16. Krenning EP, Kwekkeboom DJ, Bakker WH, et al. Somatostatin receptor scintigraphy with [<sup>111</sup>In-DTPA-D-Phe<sup>1</sup>]-and [<sup>123</sup>I-Tyr<sup>3</sup>]-octreotide: the Rotterdam experience with more than 1000 patients. *Eur J Nucl Med* 1993;20:716-31.
17. Andersson P, Forssell-Aronsson E, Johanson V, et al. Internalization of indium-111 into human neuroendocrine tumor cells after incubation with indium-111-DTPA-D-Phe<sup>1</sup>-octreotide. *J Nucl Med* 1996;37:2002-6.
18. Krenning EP, Valkema R, Kooij PPM, et al. Peptide receptor radionuclide therapy with [indium-111-DTPA-D-Phe]-octreotide. [abstract] *J Nucl Med* 1997;38(Suppl.):47P
19. Klijn JGM, Berns PMJJ, Schmitz PIM, Foekens JA. The clinical significance of epidermal growth factor receptor (EGF-R) in human breast cancer: a review on 5232 patients. *Endocr Rev* 1992;13:3-17.
20. Fields Jones SM, Burris III HA, Herfindal ET, Gourley DR. Breast Cancer. In: Herfindal ET and Gourleey DR, eds. *Textbook of Therapeutics: Drug and Disease Management*. 6th ed. Baltimore: Williams & Wilkins; 1996; 80: 1533-47.
21. Reilly RM, Gariépy J. Factors influencing the sensitivity of tumour imaging using a receptor-binding radiopharmaceutical. *J Nucl Med* 1998;39:1037-42.
22. Olsson P, Lindstrom A, Carlsson J. Internalization and excretion of epidermal growth factor-dextran-associated radioactivity in cultured human squamous-carcinoma cells. *Int J Cancer* 1994;56:529-37.

23. Rakowicz-Szulczynska EM, Rodeck U, Herlyn M, Koprowski H. Chromatin binding of epidermal growth factor, nerve growth factor, and platelet-derived growth factor in cells bearing the appropriate surface receptors. *Proc Natl Acad Sci USA* 1986;83:3728-32.
24. Filmus J, Pollak MN, Cailleau R, Buick RN. A human breast cancer cell line with a high number of epidermal growth factor (EGF) receptors, has an amplified EGF receptor gene and is growth inhibited by EGF. *Biochem Biophys Res Commun* 1985;128:898-905.
25. Dunn WA, Hubbard AL. Receptor-mediated endocytosis of epidermal growth factor by hepatocytes in the perfused rat liver: ligand and receptor dynamics. *J Cell Biol* 1984;98:2148-59.
26. Fisher DA, Salido EC, Barajas L. Epidermal growth factor and the kidney. *Annu Rev Physiol* 1989;51:67-80.
27. Osborne CK, Hamilton B, Nover M. Receptor binding and processing of epidermal growth factor by human breast cancer cells. *J Clin Endocrinol Metab* 1982;55:86-93.
28. Holt SJ, Alexander P, Inman CB, Davies DE. Ligand-induced translocation of epidermal growth factor receptor to the nucleus of NR6/HER fibroblasts is serum dependent. *Exper Cell Res* 1995;217:554-8.
29. Raper SE, Burwen SJ, Barker ME, Jones AL. Translocation of epidermal growth factor to the hepatocyte nucleus during rat liver regeneration. *Gastroenterology* 1987;92:1243-50.
30. Rakowicz-Szulczynska EM, Otwiaska D, Rodeck U, Koprowski H. Epidermal growth factor (EGF) and monoclonal antibody to cell EGF surface receptor bind to the same chromatin receptor. *Arch Biochem Biophys* 1989;268:456-64.
31. Johnson LK, Vlodavsky I, Baxter JD, Gospodarowicz D. Nuclear accumulation of epidermal growth factor in cultured rat pituitary cells. *Nature* 1980;28:340-3.
32. Laduron PM. Genomic pharmacology: more intracellular sites for drug action. *Biochem Pharmacol* 1992;44:1233-42.
33. Faraggi M, Gardin I, de Labriolle-Vaylet C, Moretti J-L, Bok BD. The influence of tracer localization on the electron dose rate delivered to the cell nucleus. *J Nucl Med* 1994;35:113-9.

34. Goddu SM, Howell RW, Rao DV. Cellular dosimetry: Absorbed fractions for monoenergetic electron and alpha particle sources and S-values for radionuclides uniformly distributed in different cell compartments. *J Nucl Med* 1994;35:303-16.
35. Wordsworth OJ, Dykes PW. A functional and morphological study of liver radiation injury following intravenous injection with colloidal gold ( $^{198}\text{Au}$ ). *Int J Radiat Biol* 1969;14:497-515.
36. Hebard DW, Jackson KL, Christensen GM. The chronological development of late radiation injury in the liver of the rat. *Radiat Res* 1980;81:441-54.
37. Waltz TM, Malm C, Nishikawa BK, Wasteson A. Transforming growth factor-alpha (TGF-alpha) in human bone marrow: demonstration of TGF-alpha in erythroblasts and eosinophilic precursor cells and of epidermal growth factor receptors in blastlike cells of myelomonocytic origin. *Blood* 1995;85:2385-92.
38. Reilly RM, Kiarash R, Sandhu J, Gariépy J. A comparison of the native peptide ligand and a monoclonal antibody against the epidermal growth factor receptor (EGFR) for imaging human breast cancer. [abstract]. *J Nucl Med* 1998;39:77P.
39. Reubi JC, Waser B, Foekens JA, Klijn JGM, Lamberts SWJ, Laissue J. Somatostatin receptor incidence and distribution in breast cancer using receptor autoradiography: relationship to EGF receptors. *Int J Cancer* 1990;46:416-20.
40. McLaughlin WH, Milius RA, Pillai KMR, Edasery JP, Blumenthal RD, Bloomer WD. Cytotoxicity of receptor-mediated 16a-[ $^{125}\text{I}$ ]iodo-estradiol in cultured MCF-7 human breast cancer cells. *J Natl Cancer Inst* 1989;81:437-40.

## LEGENDS FOR FIGURES

**FIGURE 1.** Fluorescence microscopy of MDA-MB-468 human breast cancer cells incubated with fluorescein-hEGF for 1 hour at 37 °C (left) and with the nuclear stain, 4'6'-diamidino-2-phenylindole dihydrochloride (DAPI) (right). Fluorescein-hEGF was rapidly internalized into the cytoplasm of the MDA-MB-468 cells and formed a ring surrounding the cell nucleus. The cell nucleus was visualized using DAPI.

**FIGURE 2.** Cell survival curves measured in a clonogenic assay for MDA-MB-468 (●) or MCF-7 (○) human breast cancer cells treated *in vitro* with  $^{111}\text{In}$ -DTPA-hEGF. Survival curves are also presented for MDA-MB-468 cells treated with  $^{111}\text{In}$ -DTPA-hEGF adjusted for the proportion of radioactivity localized in the cytoplasm (◆) or bound to chromatin (■). The error bars represent the s.e.m. of the surviving fraction calculated from experiments performed in triplicate dishes.

**FIGURE 3.** Alanine aminotransferase (ALT) concentrations in the plasma of Balb/c mice prior to tail vein injection (PRE) and as a function of time after injection and increasing amounts of injected  $^{111}\text{In}$ -DTPA-hEGF (3.7-44 MBq). Only at the highest administered amount of radioactivity was there a slight rise in ALT concentrations.

**FIGURE 4.** Electron micrographs of sections of liver (left) and kidney (right) of athymic mice 7 weeks after tail vein injections of two separate amounts of  $^{111}\text{In}$ -DTPA-hEGF (37 and 74 MBq) separated by a 4-week time interval. No evidence of morphological damage to the liver such as mitochondrial changes, proliferation of smooth endoplasmic reticulum or lysosomes or steatosis could be observed. Similarly, there was no apparent morphological damage to the kidneys in the form of altered renal tubular structures.

**TABLE 1**  
Kinetics of binding and internalization of  $^{111}\text{In}$ -DTPA-hEGF  
in MDA-MB-468 human breast cancer cells.

Time (h)	Proportion of $^{111}\text{In}$ -DTPA-hEGF bound to MDA-MB-468 cells (%)*	Proportion of cell-bound $^{111}\text{In}$ -DTPA-hEGF internalized by MDA-MB-468 cells (%)*
0.25	41.6 $\pm$ 6.8	66.9 $\pm$ 2.9
0.5	42.9 $\pm$ 7.6	66.2 $\pm$ 3.7
1	45.6 $\pm$ 8.8	67.4 $\pm$ 2.4
2	46.2 $\pm$ 9.1	73.1 $\pm$ 1.5
3	48.1 $\pm$ 10.0	73.0 $\pm$ 2.7
4	42.8 $\pm$ 8.4	78.3 $\pm$ 2.2
24	56.1 $\pm$ 7.4	78.6 $\pm$ 7.5

\*Mean  $\pm$  s.e.m. of 3-6 experiments.

**TABLE 2**  
Kinetics of nuclear localization of  $^{111}\text{In}$ -DTPA-hEGF  
in MDA-MB-468 breast cancer cells.

Time (h)	Proportion of cell-bound $^{111}\text{In}$ -DTPA-hEGF bound to the cell nucleus (%)*	Proportion of cell-bound $^{111}\text{In}$ -DTPA-hEGF associated with the chromatin (%)*
0.5	7.2 $\pm$ 0.8	2.5 $\pm$ 1.4
1	8.2 $\pm$ 0.5	2.9 $\pm$ 0.9
2	7.1 $\pm$ 2.2	3.4 $\pm$ 1.1
4	8.2 $\pm$ 1.0	3.6 $\pm$ 0.6
24	15.5 $\pm$ 2.1	9.6 $\pm$ 1.3

\*Mean  $\pm$  s.e.m. of 3 experiments.

**TABLE 3**  
Inhibition of the growth of human breast cancer cells by treatment *in vitro* with  $^{111}\text{In}$ -DTPA-hEGF.

MDA-MB-468 Cells				MCF-7 Cells		
Treatment:	None	DTPA-hEGF	<sup>111</sup> In-DTPA	<sup>111</sup> In-DTPA-hEGF	None	<sup>111</sup> In-DTPA-hEGF
1 day	2.9 ± 0.2	3.5 ± 0.2	3.3 ± 0.4	4.1 ± 0.2	4.0 ± 0.7	4.2 ± 0.3
7 days	10.6 ± 0.9	8.6 ± 0.3	10.1 ± 0.9	5.2 ± 0.2	6.5 ± 1.0	10.4 ± 0.5
Growth Index†:	3.7 ± 0.2	2.5 ± 0.2 ‡	3.1 ± 0.1 ¶	1.3 ± 0.1**	1.7 ± 0.4	2.5 ± 0.3 ¶

\* Mean  $\pm$  s.e.m. of 3-6 replicates.

† Number of cells recovered at day 7 divided by number of cells recovered at day 1.

‡ Significantly different from untreated cells ( $p = 0.008$ ).

¶ Not significantly different from untreated cells.

\*\* Significantly different from untreated cells ( $p < 0.0001$ ).

TABLE 4

Radiation absorbed dose estimates to the cell nucleus by  $^{111}\text{In}$ -DTPA-hEGF localized in compartments of a MDA-MB-468 human breast cancer cell\*.

Cell compartment	$\tilde{A}$ (Bq.sec)‡	S (Gy/Bq.sec X $10^{-4}$ )	Radiation dose to the cell nucleus†
			$\bar{D}$ (Gy)
Membrane	3,357	1.78	0.60
Cytoplasm	10,917	3.18	3.47
Nucleus	2,522	60.30	15.21
		Total:	19.28

\*The cellular radiation dosimetry model of Goddu et al. J. Nucl. Med. 35: 303-316, 1994 was used to estimate the radiation absorbed dose ( $\bar{D}$ ) to the cell nucleus:  $\bar{D} = \tilde{A} \cdot S$  where S is the radiation absorbed dose in the nucleus (Gy) per unit of cumulated radioactivity in the source compartment,  $\tilde{A}$  (Bq.sec).

†Based on targeting a single MDA-MB-468 human breast cancer cell with a diameter of 10 mm and a nucleus with a diameter of 6 mm to receptor saturation with  $^{111}\text{In}$ -DTPA-hEGF. At concentrations of the radioligand leading to receptor saturation, approximately 48 mBq of  $^{111}\text{In}$ -DTPA-hEGF would be bound to each MDA-MB-468 cell at a specific activity of 3.7 MBq/mg.

‡Assumes the rapid localization of  $^{111}\text{In}$ -DTPA-hEGF in a compartment and a rate of elimination corresponding to the radioactive decay of the radionuclide, indium-111.  $\tilde{A} = A_0 / \lambda$ , where  $\lambda$  is the radioactive decay constant for  $^{111}\text{In}$  ( $2.83 \times 10^{-6} \text{ sec}^{-1}$ ).

TABLE 5

Biodistribution of  $^{111}\text{In}$ -DTPA-hEGF at 72 hours post-injection in athymic mice bearing subcutaneous MDA-MB-468 human breast cancer xenografts\*.

Tissue	Localization of $^{111}\text{In}$ -DTPA-hEGF	
	†Percent injected dose/g	†Tumour/Normal Tissue Ratio
Blood	$0.19 \pm 0.03$	$11.85 \pm 1.10$
Heart	$0.57 \pm 0.03$	$3.92 \pm 0.50$
Lungs	$0.89 \pm 0.07$	$2.52 \pm 0.28$
Liver	$9.97 \pm 0.07$	$0.28 \pm 0.08$
Kidneys	$13.69 \pm 1.51$	$0.18 \pm 0.04$
Spleen	$2.29 \pm 0.19$	$0.98 \pm 0.11$
Stomach	$0.54 \pm 0.05$	$4.46 \pm 0.97$
Intestine	$1.77 \pm 0.24$	$1.45 \pm 0.38$
Tumour	$2.24 \pm 0.32$	na

\*Abstracted from: Reilly RM, Kiarash R, Sandhu JS et al. A comparison of epidermal growth factor and monoclonal antibody 528 labeled with indium-111 for imaging breast cancer. *J Nucl Med* (submitted) 1999.

† Mean  $\pm$  s.e.m. (n = 5)

*Figures available on request.*

## **A Comparison of Epidermal Growth Factor and Monoclonal Antibody 528 Labeled with Indium-111 for Imaging Human Breast Cancer**

Raymond M. Reilly, Ph.D., Reza Kiarash, B.Sc., Jasbir Sandhu, Ph.D., Ying Wai Lee, B.Sc.Pharm., Ross G. Cameron, M.D., Ph.D., Aaron Hendler, M.D., Katherine Vallis, M.D., Ph.D. and Jean Gariépy, Ph.D.

*Division of Nuclear Medicine (R.M.R., R.K., Y.W.L., A.H.) and Departments of Pathology (R.G.C.) and Radiation Oncology (K.V.), The Toronto Hospital/Princess Margaret Hospital; Samuel Lunenfeld Research Institute, Mount Sinai Hospital (J.S.); Departments of Medical Imaging (R.M.R., A.H.), Pharmaceutical Sciences (R.M.R.), Radiation Oncology (K.V.) and Medical Biophysics (R.M.R., K.V., J.G.) University of Toronto.*

Address correspondence and requests for reprints to:

Raymond M. Reilly and Jean Gariépy  
Division of Nuclear Medicine, The Toronto Hospital  
585 University Avenue  
Toronto, ON, Canada  
M5G 2C4  
Tel.: (416) 340-3036  
FAX: (416) 340-5065  
e-mail: raymond.reilly@utoronto.ca

This research was supported in part by grants from DuPont Pharma, the Susan G. Komen Breast Cancer Foundation (Grant No. 9749) and the U.S. Army Breast Cancer Research Program (Grant No. DAMD17-98-1-8171) to R.M.R. and a grant from the National Cancer Institute of Canada with funds from the Canadian Cancer Society to J.G. Parts of this study were presented at the Society of Nuclear Medicine 45th Annual Meeting, Toronto, June 8, 1998.

Running Footline: Imaging of Breast Cancer Xenografts  
Revised July 20, 1999

## ABSTRACT

Our objective was to compare  $^{111}\text{In}$ -labeled human epidermal growth factor (hEGF), a 53-amino acid peptide with anti-EGFR monoclonal antibody (mAb) 528 (IgG<sub>2a</sub>) for imaging EGFR-positive breast cancer. **Methods:** hEGF and mAb 528 were derivatized with diethylenetriaminepentaacetic acid (DTPA) and labeled with  $^{111}\text{In}$  acetate. Receptor binding assays were conducted *in vitro* against MDA-MB-468 human breast cancer cells. Biodistribution and tumor imaging studies were conducted following i.v. injection of the radiopharmaceuticals in athymic mice bearing s.c. MCF-7, MDA-MB-231 or MDA-MB-468 human breast cancer xenografts or in *scid* mice implanted with a breast cancer metastasis (JW-97 cells). MCF-7, MDA-MB-231, JW-97 and MDA-MB-468 cells expressed  $1.5 \times 10^4$ ,  $1.3 \times 10^5$ ,  $2.7 \times 10^5$  and  $1.3 \times 10^6$  EGFR/cell respectively *in vitro*. **Results:**  $^{111}\text{In}$ -DTPA-hEGF and  $^{111}\text{In}$ -DTPA-mAb 528 bound with high affinity to MDA-MB-468 cells ( $K_a$  of  $7.5 \times 10^8$  and  $1.2 \times 10^8$  L/mol respectively).  $^{111}\text{In}$ -DTPA-hEGF was eliminated rapidly from the blood with  $<0.2\%$  injected dose/g (% i.d./g) circulating at 72 hours p.i. whereas  $^{111}\text{In}$ -DTPA-mAb 528 was cleared more slowly (3% i.d./g in the blood at 72 hours). Maximum localization of  $^{111}\text{In}$ -DTPA-hEGF in MDA-MB-468 tumours (2.2% i.d./g) was 10-fold lower than with  $^{111}\text{In}$ -DTPA-mAb 528 (21.6% i.d./g). There was high uptake in the liver and kidneys for both radiopharmaceuticals. Tumor/blood ratios were greater for  $^{111}\text{In}$ -labelled hEGF than for mAb 528 (12:1 versus 6:1) but all other tumor/normal tissue ratios were higher for mAb 528. MDA-MB-468 and JW-97 tumors were successfully imaged with either radiopharmaceutical but tumors were more easily visualized using  $^{111}\text{In}$ -labeled mAb 528. There was no direct quantitative relationship between EGFR expression on breast cancer cell lines *in vitro*, and tumor uptake of the radiopharmaceuticals *in vivo* but control studies demonstrated that tumor uptake was receptor-mediated. **Conclusion:** Our results suggest that the tumor uptake *in vivo* of receptor-binding radiopharmaceuticals is controlled to a greater extent by their elimination rate from the blood than by the level of receptor expression on the cancer cells. Radiolabeled anti-EGFR mAbs would be more effective for tumor imaging in cancer patients than peptide-based radiopharmaceuticals such as hEGF, because they exhibit higher tumor uptake at only moderately lower tumor/blood ratios.

**Key words:** breast cancer; epidermal growth factor; monoclonal antibody 528; indium-111; imaging; epidermal growth factor receptor

## INTRODUCTION

The overexpression of cell surface receptors for peptide growth factors is believed to be one process whereby cancer cells acquire the ability to escape normal growth regulatory mechanisms. The presence of the epidermal growth factor receptor (EGFR) at levels up to 100 times higher than on most normal epithelial tissues ( $<10^4$  receptors/cell) has been observed in 30-60% of human breast cancers (reviewed in (1)). EGFR overexpression in breast cancer is inversely correlated with estrogen receptor (ER) expression and is directly correlated with a lack of response to hormonal therapy with tamoxifen. Several studies have associated this cellular phenotype with a poor long-term survival (1).

Patients with disseminated, hormone-resistant breast cancer are candidates for systemic chemotherapy. In addition, new drugs are currently under development which would specifically target the high levels of EGFR expression commonly observed in such malignancies. These drugs include monoclonal antibodies (mAbs) which block the binding of epidermal growth factor (EGF) to the receptor (2), tyrosine kinase inhibitors (tyrphostins) which can interfere with the intracellular signaling pathways (3), and EGF-conjugated toxins which specifically deliver highly potent inhibitors of protein synthesis into the cytoplasm of the cancer cells (4). A logical extension of this strategy, currently being explored in our laboratory (5) and by others (6), would be to develop novel radiotherapeutic agents which could deliver high doses of radiation specifically to EGFR-positive cancer cells.

The effectiveness of new therapeutic agents targeted to the EGF receptor will depend on the ability to detect and characterize EGFR expressing metastatic lesions throughout the body. ER status is commonly measured in biopsies of primary breast cancer lesions at the time of staging in order to select patients for hormonal therapy. EGFR expression in metastatic disease could be inferred from the inverse correlation between ER and EGFR expression in breast cancer. This approach may be limited however by potential differences in EGFR/ER positivity between the primary tumor and metastases, heterogeneity in receptor expression by the tumor cells, temporal changes in ER/EGFR expression which can occur as a result of treatment (7) and the inability to directly evaluate EGFR expression in individual lesions. A survey of the whole body by gamma scintigraphy using radiopharmaceuticals specifically targeted to the EGFR would be useful to detect breast cancer lesions and characterize the level of EGFR expression at these sites in order to appropriately select patients for novel anti-EGFR therapies.

It has been proposed (8) that peptide-based radiopharmaceuticals such as radiolabeled growth factors may be more effective for imaging of tumors than radiolabeled mAbs due to their more rapid elimination from the blood which produces higher tumor/blood ratios at early time points. The objective of this

study was therefore to directly compare human epidermal growth factor (hEGF), a 53-amino acid peptide ligand for the EGFR with anti-EGFR mAb 528 (9) labeled with indium-111 ( $^{111}\text{In}$ ) for imaging EGFR-positive human breast cancer.

## MATERIALS AND METHODS

### Breast cancer cells

MDA-MB-468 and MDA-MB-231 human breast cancer cells were obtained from the American Type Culture Collection (ATCC, Rockville, MD) and were cultured in L-15 medium (Sigma, St. Louis, MO) supplemented with 10% fetal calf serum (FCS). MCF-7 breast cancer cells were obtained from Dr. A. Marks at the Banting and Best Department of Medical Research, University of Toronto and were cultured in Minimal Essential Medium (MEM, Sigma, St. Louis, MO) supplemented with 10% FCS, non-essential amino acids and glutamine (Gibco-BRL, Life Technologies, Burlington, ON, Canada). S1 breast cancer cells are a subclone of the MDA-MB-468 breast cancer cell line which express a lower number of EGFR molecules on their surface (10). S1 cells were obtained from Dr. R. Buick at the Ontario Cancer Institute and were cultured in L-15 medium supplemented with 10% FCS and  $10^{-7}$  M EGF. JW-97 human breast cancer cells were obtained by trypsinization of a skeletal metastasis from a patient with advanced disease which was passaged in severe combined immunodeficiency (*scid*) mice. JW-97 cells were cultured in RPMI 1640 medium (Sigma, St. Louis, MO) supplemented with 10% FCS.

### Radiolabelling of epidermal growth factor

hEGF (Upstate Biotechnology, Lake Placid, NY) was derivatized with diethylenetriaminepentaacetic acid (DTPA) using the bicyclic anhydride of DTPA (Sigma, St. Louis, MO) as previously described (11). DTPA-derivatized hEGF demonstrated a single band with an apparent  $M_r$  of 6 kDa by sodium dodecylsulfate polyacrylamide gel electrophoresis (SDS-PAGE) on a Tris-Tricine gel (BioRad, Mississauga, ON, Canada) indicating no apparent cross-linking of hEGF molecules following reaction with the bicyclic DTPA anhydride. DTPA-conjugated hEGF (25-50 mg) was radiolabeled with  $^{111}\text{In}$  acetate to a specific activity of 3.7-7.4 MBq/mg (22,200-44,400 MBq/mmol).  $^{111}\text{In}$  acetate was prepared by mixing equal volumes of  $^{111}\text{In}$  chloride ( $>7,400$  MBq/mL, MDS-Nordion, Kanata, ON, Canada) and 1 M acetate buffer pH 6.  $^{111}\text{In}$ -DTPA-hEGF was purified from free  $^{111}\text{In}$  by size-exclusion chromatography on a P-2 mini-column (BioRad, Mississauga, ON, Canada), then analyzed for radiochemical purity by silica gel instant thin layer chromatography (ITLC-SG, Gelman, Ann Arbor, MI) in 100 mM sodium citrate pH 5. The radiolabelling efficiency was approximately 80%. The radiochemical purity of  $^{111}\text{In}$ -DTPA-hEGF was routinely between 95-98%.

hEGF was radioiodinated to a specific activity of 1.5-2.2 MBq/mg (8,880-13,320 mCi/mmol) by incubating 10 mg of hEGF with 18.5-37 MBq of  $^{125}\text{I}$  sodium iodide (Nycomed-Amersham, Oakville, ON, Canada) and 20 mg of chloramine-T (Sigma, St. Louis, MO) for 30 seconds in a glass tube at room temperature. After addition of sodium metabisulfite (40 mg), the radioiodinated hEGF was purified on a P-2 mini-column. The radiolabelling efficiency was approximately 70%. The radiochemical purity of  $^{125}\text{I}$ -hEGF was >95% as determined by paper chromatography (Whatman No. 1, Maidstone, England) in 85% methanol.

### **Production and radiolabeling of monoclonal antibody 528**

HB 8509 hybridoma cells secreting anti-EGFR mAb 528 (IgG<sub>2a</sub>) were obtained from ATCC (Rockville, MD) and were cultured in RPMI 1640 supplemented with 20% FCS. Balb/c mice were injected i.p. with 1 mL of Pristane (2,6,10,14-tetramethylpentadecane, Sigma, St Louis, MO) followed 3-4 days later with an i.p. injection of  $10^7$  HB 8509 hybridoma cells in culture medium. After 2 weeks, the ascites fluid was removed from the peritoneal cavity and anti-EGFR mAb 528 was purified from the ascites fluid on a Protein G column (Pierce, Rockford, IL). The purified mAb 528 was desalted on a Sephadex G-25 column (PD-10, Pharmacia, Uppsala, Sweden), concentrated on a Centricon-30 ultrafiltration device (Amicon, Beverly, MA) and diluted to a concentration of 10 mg/mL in 50 mM sodium bicarbonate buffer pH 7.5. The purity of the mAb 528 preparation was assessed by SDS-PAGE under non-reducing conditions on a 4-20% Tris-glycine gel (BioRad). The protein preparation resulted in a single band migrating with an apparent molecular weight ( $M_r$ ) of 150 kDa. Approximately 2 mg of mAb 528 was obtained per mL of ascites fluid.

Monoclonal antibody 528 (0.5-1 mg), 10 mg/mL in trace-metal free 50 mM sodium bicarbonate buffer pH 7.5 was derivatized with DTPA using the bicyclic anhydride of DTPA (cDTPAA, Sigma, St. Louis, MO) at a molar ratio (cDTPAA:mAb 528) of 10:1 as previously described (12). DTPA-mAb 528 was purified by size-exclusion chromatography on a Sephadex G-50 (Pharmacia, Uppsala, Sweden) mini-column eluted with 50 mM sodium bicarbonate buffer pH 7.5 followed by ultrafiltration through a Centricon-30 device. Analysis of DTPA-mAb 528 by SDS-PAGE under non-reducing conditions on a 4-20% Tris-glycine gel (BioRad) showed a predominant band with an apparent  $M_r$  of 150 kDa and a minor band with apparent  $M_r$  of 300 kDa, indicating a small proportion (<10%) of mAb 528 molecules cross-linked through the bicyclic DTPA anhydride. DTPA-mAb 528 (250-500 mg) was radiolabeled to a specific activity of 0.07-0.14 MBq/mg (11,100-22,200 MBq/mmol) with  $^{111}\text{In}$  acetate (37 MBq) and purified from free  $^{111}\text{In}$  on a Sephadex G-50 mini-column eluted with 150 mM sodium chloride. The radiolabelling efficiency of DTPA-mAb 528 was approximately 85%. The radiochemical purity of  $^{111}\text{In}$ -DTPA-mAb 528 was routinely >95%.

determined by ITLC-SG developed in 100 mM sodium citrate pH 5. A non-specific murine IgG<sub>2a</sub> (Sigma Product No. M-9144, St. Louis, MO) was derivatized with cDTPAA and radiolabeled with <sup>111</sup>In acetate in an identical manner to mAb 528.

Monoclonal antibody 528 (25-50 mg) was radioiodinated to a specific activity of 0.18-0.37 MBq/mg (27,750-55,500 MBq/mmol) by incubation with 18.5 MBq <sup>125</sup>I sodium iodide in a glass tube pre-coated with 20 mg of 1,3,4,6-tetrachloro-3a,6a-diphenylglycouril (Sigma, St. Louis, MO) at room temperature. Radioiodinated mAb 528 was purified on a Sephadex G-50 mini-column. The radiolabelling efficiency was approximately 70%. The radiochemical purity of <sup>125</sup>I-mAb 528 was >95% as determined by paper chromatography (Whatman No. 1) in 85% methanol.

### Measurement of receptor binding *in vitro*

The binding of radiolabeled hEGF or mAb 528 to its receptor on MDA-MB-468, S1, MDA-MB-231, MCF-7 or JW-97 human breast cancer cells was measured using a direct binding assay. Briefly, aliquots of either radiolabeled hEGF (0.25-80 ng) or mAb 528 (6 ng-4 mg) were dispensed into 35 mm multiwell culture dishes containing 1.5 to 7 X 10<sup>6</sup> breast cancer cells in 1 mL of 150 mM sodium chloride containing 0.2% w/v human serum albumin. After incubation of the dishes at 37 °C for 30 minutes, the cells were transferred to tubes and centrifuged to separate the bound radioactivity (B) in the cell pellet from the free radioactivity (F) in the supernatant. The cell pellet and supernatant were counted in a gamma scintillation counter (Packard Auto Gamma 5650, Packard Instruments, Downer's Grove, IL). Non-specific binding was determined by conducting the assay in the presence of 100 nM hEGF or mAb 528. The affinity constant ( $K_a$ ) and number of receptors/cell ( $B_{max}$ ) were determined from a non-linear fitting of the binding data (13).

The receptor-binding fraction (RBF) at infinite receptor excess was determined by incubating 0.5-1 ng of <sup>111</sup>In-DTPA-hEGF or 10-20 ng of <sup>111</sup>In-DTPA-mAb 528 with increasing concentrations of MDA-MB-468 breast cancer cells (1 to 20 X 10<sup>6</sup> cells/mL) for 30 minutes at 37 °C and determining the fraction of radioactivity bound. The RBF at infinite receptor excess was obtained from the intercept on the ordinate (1/RBF) of a plot of total/bound counts versus 1/cell concentration as previously described by Lindmo et al. (14).

### Biodistribution and tumor imaging studies

Four to six weeks old female, Swiss athymic (*nu/nu*) mice (Charles River Laboratories, Montreal, PQ, Canada) were injected subcutaneously in the right hind leg with 5 X 10<sup>6</sup> to 10<sup>7</sup> MDA-MB-468, MDA-MB-231 or MCF-7 human breast cancer cells in growth medium. Mice inoculated with MCF-7 cells also received estradiol supplementation with bi-weekly s.c. injections of 0.5 mg of conjugated

estrogens (Premarin®, Wyeth-Ayerst, St. Laurent, PQ, Canada) required for MCF-7 cells to form tumor xenografts. A freshly obtained biopsy of a skeletal metastasis from a patient with advanced breast cancer (JW-97 cells) was implanted in the left hind leg of *scid* mice (Samuel Lunenfeld Research Institute). A dose of 1.85-3.7 MBq of  $^{111}\text{In}$ -DTPA-hEGF (0.5-1 mg) or  $^{111}\text{In}$ -DTPA-mAb 528 (25-50 mg) was injected i.v. into mice when the tumors reached a diameter of 0.25-0.5 cm (1-2 cm for JW-97 tumors). One group of control mice received a dose of 1.85-3.7 MBq of  $^{111}\text{In}$ -DTPA (DraxImage, Dorval, PQ). An  $^{111}\text{In}$ -labeled non-specific murine IgG<sub>2a</sub> was injected into a second group of control mice while  $^{111}\text{In}$ -DTPA-hEGF pre-mixed with 500 mg of non-radioactive hEGF (ratio of non-radioactive hEGF: $^{111}\text{In}$ -DTPA-hEGF = 1000:1) was injected i.v. into a third group of control mice.

At 24, 48 and 72 hours post-injection, groups of mice were sacrificed by cervical dislocation and the tumor and samples of normal tissues were removed to measure levels of radioactivity. Tissue samples were weighed and counted along with a standard of the injected radiopharmaceutical in a gamma counter (Packard Auto Gamma 5650, Packard Instruments, Downer's Grove, IL) using a window (150-270 keV) to include the two gamma photopeaks of  $^{111}\text{In}$  (172, 247 keV). The uptake of each radiopharmaceutical by the tumor and normal tissue was expressed as percent injected dose per gram of tissue (% i.d./g) and as tumor/normal tissue (T/NT) ratios. At 72 hours post-injection, posterior images of the mice implanted with the MDA-MB-468, JW-97 or MCF-7 human breast cancer xenografts were obtained on a Siemens ZLC-3700 gamma camera (Siemens, Knoxville, TN) fitted with a medium energy pinhole collimator and interfaced to a General Electric Star 4000i computer (General Electric, Milwaukee, WI). Images were acquired for 10 minutes using a 20% window centered over the 172 and 247 keV photopeaks of  $^{111}\text{In}$ . Animal studies were conducted under an approved Animal Care Protocol (# 94-036) at The Toronto Hospital and following the Canadian Council on Animal Care (CCAC) guidelines.

### Statistical analysis

Statistical comparisons were performed by ANOVA (F-test,  $p < 0.05$ ) and Student's t-test ( $p < 0.05$ ).

## RESULTS

### Binding of radiolabeled hEGF and mAb 528 to breast cancer cells *in vitro*

$^{111}\text{In}$ -DTPA-hEGF and  $^{111}\text{In}$ -DTPA-mAb 528 bound with high affinity and specificity *in vitro* to MDA-MB-468 human breast cancer cells (Table 1). The affinity constant ( $K_a$ ) was approximately 6-fold higher for  $^{111}\text{In}$ -DTPA-hEGF than for  $^{111}\text{In}$ -DTPA-mAb 528. There was no significant difference in binding affinity between the  $^{111}\text{In}$  and corresponding  $^{125}\text{I}$  labeled analogs, suggesting that the

conjugation of the DTPA chelator to amino groups and their radiolabelling with  $^{111}\text{In}$  did not adversely effect the binding of the resulting radiopharmaceutical to the EGFR. The number of binding sites recognized on the MDA-MB-468 cells ( $B_{\text{max}}$ ) was similar for all four radiolabeled ligands. There was no significant difference ( $p = 0.0847$ ) in the fraction of radiolabelled molecules able to bind to EGF receptors on MDA-MB-468 cells under conditions of infinite receptor excess (receptor-binding fraction, RBF) for  $^{111}\text{In}$ -DTPA-hEGF ( $0.73 \pm 0.17$ ,  $n = 3$ ) and  $^{111}\text{In}$ -DTPA-mAb 528 ( $0.50 \pm 0.04$ ,  $n = 3$ ).

EGFR expression varied considerably among the five breast cancer cell lines tested (Table 2). The highest expression ( $>10^6$  EGFR/cell) was observed on MDA-MB-468 cells which have an amplified EGFR gene (10). MCF-7 and S1 cells exhibited the lowest expression ( $<10^4$  EGFR/cell). MCF-7 is an ER-positive cell line, expected to have low EGFR expression and the cell line S1 represents a subclone of the MDA-MB-468 cell line, where the expression of the EGFR gene is down-regulated (10). JW-97 cells, originally obtained from a biopsy of a skeletal metastasis in a patient with advanced disease, exhibited intermediate levels of EGFR expression, similar to the levels on the MDA-MB-231 breast cancer cell line ( $1-3 \times 10^5$  receptors/cell) but almost 30-fold higher than on most normal epithelial tissues ( $<10^4$  EGFR/cell).

#### **Biodistribution and tumor imaging studies**

The biodistribution of  $^{111}\text{In}$ -DTPA-hEGF and  $^{111}\text{In}$ -DTPA-mAb 528 at selected times after an i.v. (tail vein) injection in athymic mice bearing subcutaneous MDA-MB-468 human breast cancer xenografts is shown in Fig. 1. The blood levels of  $^{111}\text{In}$ -DTPA-hEGF (Fig. 1 A) decreased rapidly with  $<0.8\%$  i.d./g present in the blood at 24 hours post-injection decreasing to  $<0.2\%$  i.d./g at 72 hours. Assuming a blood volume of approximately 2.5 mL for a mouse weighing 25 g, the concentration of  $^{111}\text{In}$ -DTPA-hEGF in the blood corresponded to about 1.7-2.5% of the injected dose of the radiopharmaceutical at 24 hours and  $<0.5\%$  at 72 hours. In contrast, the blood levels of  $^{111}\text{In}$ -DTPA-mAb 528 (Fig. 1 B) decreased more slowly with approximately 9% i.d./g present in the blood at 24 hours post-injection decreasing to 3% i.d./g at 72 hours. The concentration of  $^{111}\text{In}$ -DTPA-mAb 528 in the blood corresponded to about 21-25% of the injected dose of the radiopharmaceutical circulating at 24 hours post-injection decreasing to about 7-8% at 72 hours.

The normal tissues which accumulated the highest concentrations of the radiopharmaceuticals were the liver and kidneys (Fig. 1). Liver uptake of  $^{111}\text{In}$ -DTPA-hEGF (Fig. 1 A) was relatively constant ranging from 8-10% i.d./g. The concentration of  $^{111}\text{In}$ -DTPA-hEGF in the kidneys increased slightly from about 11% i.d./g at 24 hours to 14% i.d./g at 72 hours post-injection. Approximately 11-14% of the injected dose of  $^{111}\text{In}$ -DTPA-hEGF localized in the liver and 4-5% in the kidneys assuming organ weights of 1.4 g and 0.36 g respectively. For  $^{111}\text{In}$ -

DTPA-mAb 528 (Fig. 1 B), liver accumulation ranged from 6-8% i.d./g and uptake in the kidneys was 12-17% i.d./g over the time period of 24 to 72 hours post-injection. The liver sequestered approximately 8-11% of the injected dose of  $^{111}\text{In}$ -DTPA-mAb 528 and the kidneys accumulated 4-6%. There were no significant differences in the concentration of the two radiopharmaceuticals in the liver or kidneys at 72 hours.

Maximum localization of  $^{111}\text{In}$ -DTPA-hEGF in the MDA-MB-468 human breast cancer xenografts occurred at 72 hours post-injection (2.2% i.d./g) and was up to 10-fold lower than that observed for  $^{111}\text{In}$ -DTPA-mAb 528 (Fig. 1). Maximum tumor uptake of  $^{111}\text{In}$ -DTPA-mAb 528 occurred at 24 hours post-injection (21.6% i.d./g) then decreased to 11-15% i.d./g at 48 to 72 hours post-injection. The mean uptake of  $^{111}\text{In}$ -DTPA-hEGF in the MDA-MB-468 breast cancer xenografts at 72 hours post-injection was decreased more than 5-fold by co-administering 500 mg of unlabeled hEGF ( $0.40 \pm 0.15$  % i.d./g) suggesting that tumor uptake was a receptor-mediated event. Similarly, the uptake of non-specific  $^{111}\text{In}$ -labeled IgG<sub>2a</sub> into MDA-MB-468 breast cancer xenografts at 72 hours post-injection ( $9.13 \pm 1.92$  % i.d./g) was 2-fold lower than that observed for  $^{111}\text{In}$ -DTPA-mAb 528 suggesting that uptake of mAb 528 by tumor cells was also receptor mediated. The mean tumor uptake of  $^{111}\text{In}$ -DTPA at 72 hours post-injection was  $0.07 \pm 0.01$  % i.d./g.

T/NT ratios at selected times after administration of the radiopharmaceuticals are shown in Fig. 2. Tumor/blood ratios increased rapidly for  $^{111}\text{In}$ -DTPA-hEGF (Fig. 2 A) reaching values of 2.6:1 at 24 hours increasing to 12:1 at 72 hours post-injection. Tumor/blood ratios for  $^{111}\text{In}$ -DTPA-mAb 528 (Fig. 2 B) increased more slowly from 2.5:1 at 24 hours to about 6:1 at 72 hours post-injection. T/NT ratios for  $^{111}\text{In}$ -DTPA-hEGF were  $>2:1$  for blood, heart, lungs, stomach and intestine up to 72 hours post-injection but were  $<1:1$  for the liver and kidneys due to high accumulation of the radiopharmaceutical in these normal tissues. Except for the blood, all other T/NT ratios for  $^{111}\text{In}$ -DTPA-mAb 528 were higher than those for  $^{111}\text{In}$ -DTPA-hEGF (Fig. 2 B). Tumor/liver ratios for  $^{111}\text{In}$ -DTPA-mAb 528 (1.4:1 to 3.3:1) were 5 to 11-fold higher than those observed for  $^{111}\text{In}$ -DTPA-hEGF and tumor/kidney ratios were 3 to 10-fold greater (0.7:1 to 1.8:1).

Biodistribution studies in athymic or *scid* mice bearing s.c. MDA-MB-468, MDA-MB-231, JW-97 or MCF-7 human breast cancer xenografts at 72 hours post-injection of  $^{111}\text{In}$ -DTPA-hEGF or  $^{111}\text{In}$ -DTPA-mAb 528 demonstrated no direct correlation between the level of tumor uptake of the radiopharmaceuticals and the level of EGFR expression on these cell lines measured *in vitro* (Table 2). For example, there were no significant differences in the level of accumulation of  $^{111}\text{In}$ -DTPA-hEGF (or  $^{111}\text{In}$ -DTPA-mAb 528) in MCF-7 or MDA-MB-468 breast cancer xenografts despite a 100-fold difference in receptor expression ( $p = 0.6408$  and  $p = 0.0957$  respectively). Similarly, there were no significant

differences in the level of accumulation of  $^{111}\text{In}$ -DTPA-hEGF (or  $^{111}\text{In}$ -DTPA-mAb 528) in MDA-MB-231 and MDA-MB-468 breast cancer xenografts despite a 10-fold difference in receptor expression ( $p = 0.3955$  and  $p = 0.6838$  respectively). Nevertheless, the tumor uptake of  $^{111}\text{In}$ -DTPA-mAb 528 was 4 to 12 fold higher than that of  $^{111}\text{In}$ -DTPA-hEGF in all cases. The localization of either  $^{111}\text{In}$ -DTPA-hEGF or  $^{111}\text{In}$ -DTPA-mAb 528 was significantly lower in JW-97 tumors than in the MDA-MB-468 breast cancer xenografts ( $p = 0.0041$  and  $p = 0.0260$  respectively). There was no significant difference in the tumor uptake of  $^{111}\text{In}$ -DTPA-hEGF in MDA-MB-231 breast cancer xenografts as compared to the JW-97 tumors ( $p = 0.427$ ). Similarly, there was no significant difference in the tumor uptake of  $^{111}\text{In}$ -DTPA-mAb 528 between the MDA-MB-231 or JW-97 tumor xenografts ( $p = 0.684$ ).

MDA-MB-468 and JW-97 human breast cancer xenografts expressing  $1.3 \times 10^6$  or  $2.7 \times 10^5$  EGF receptors/cell *in vitro* respectively (Table 1) were successfully imaged with  $^{111}\text{In}$ -DTPA-hEGF or  $^{111}\text{In}$ -DTPA-mAb 528 at 72 hours post-injection (Fig. 3 and Fig. 4). However, the greater tumor uptake of  $^{111}\text{In}$ -DTPA-mAb 528 compared to  $^{111}\text{In}$ -DTPA-hEGF resulted in an enhanced definition of the breast cancer xenografts. The liver and kidneys were the major normal organs visualized on the images but there was also some uptake in the area of the submaxillary glands. The levels of circulating radioactivity and whole body radioactivity were considerably lower on the images obtained using  $^{111}\text{In}$ -DTPA-hEGF than on those obtained with  $^{111}\text{In}$ -DTPA-mAb 528. MCF-7 xenografts could not be visualized with either  $^{111}\text{In}$ -DTPA-hEGF or  $^{111}\text{In}$ -DTPA-mAb 528 due to their small size ( $<0.2$  cm in diameter).

## DISCUSSION

Our objective was to compare a peptide-based radiopharmaceutical and a mAb directed against the same cell-surface receptor for imaging of human breast cancer. A systematic evaluation of the localization profiles of these two different radiopharmaceuticals was conducted in breast cancer xenografts expressing a broad range of EGF receptor levels. EGFR-positive breast cancer xenografts hosted in immunocompromised mice were successfully imaged using hEGF, a 53-amino acid peptide ligand ( $M_r$  6 kDa) for the receptor or anti-EGFR mAb 528 ( $M_r$  150 kDa) labeled with  $^{111}\text{In}$ . The tumor uptake observed with  $^{111}\text{In}$ -DTPA-mAb 528 was 7 to 10 fold higher than that observed for  $^{111}\text{In}$ -DTPA-hEGF. As a result, the images of the breast cancer xenografts were much clearer with  $^{111}\text{In}$ -DTPA-mAb 528, indicating that in certain situations mAbs are more effective tumor targeting vehicles than peptide growth factors for receptor imaging of cancer. The higher tumor uptake observed with  $^{111}\text{In}$ -DTPA-mAb 528 was likely due to its slower elimination from the blood which permitted a greater proportion of the injected dose of the radiopharmaceutical to diffuse into the extravascular space

and bind to receptors on breast cancer cells. The higher accumulation of radioactivity in the MDA-MB-468 breast cancer xenografts observed for  $^{111}\text{In}$ -DTPA-mAb 528 was not due to a higher receptor binding affinity, since cell binding assays demonstrated that the affinity constant for  $^{111}\text{In}$ -DTPA-mAb 528 was actually 6-fold lower than that for  $^{111}\text{In}$ -DTPA-hEGF ( $K_a = 1.2 \times 10^8$  versus  $7.5 \times 10^8$  L/mol respectively, Table 1).

$^{111}\text{In}$ -DTPA-hEGF was rapidly eliminated from the blood in the animals with <2-3% of the injected dose remaining in the circulation at 24 hours post-injection and <1% at 72 hours. Two possible mechanisms could explain the rapid blood clearance of  $^{111}\text{In}$ -DTPA-hEGF: 1) sequestration by normal tissues which have high levels of EGFR expression (eg. liver and kidneys) and 2) a high proportion of renal elimination.  $^{111}\text{In}$ -DTPA-mAb 528 was eliminated much more slowly from the blood than  $^{111}\text{In}$ -DTPA-hEGF with 25-30% of the injected dose present in the circulation at 24 hours post-injection and 10% at 72 hours. The slow elimination of  $^{111}\text{In}$ -DTPA-mAb 528 from the blood was due to its large molecular size ( $M_r$  150 kDa) which prevented its filtration at the glomerulus, a process which is restricted to proteins with  $M_r$  <60 kDa.

Normal hepatocytes exhibit moderate to high levels of EGFR expression ( $8 \times 10^4$  to  $3 \times 10^5$  EGFR/cell) (15,16) and specific receptors for  $^{125}\text{I}$ -EGF have been detected *in vitro* in rat kidney homogenates (17) and on renal tubular cells (18). The liver has also been shown to have a high capacity to extract  $^{125}\text{I}$ -EGF from the circulation (16,19).  $^{125}\text{I}$ -EGF taken up by hepatocytes is primarily internalized into lysosomes and degraded, but a fraction of internalized EGF molecules are transported by a non-lysosomal pathway and secreted into the bile (19). In our study, the liver and kidneys accumulated the highest concentrations of  $^{111}\text{In}$ -DTPA-hEGF and  $^{111}\text{In}$ -DTPA-mAb 528. Although  $^{125}\text{I}$ -labeled EGF has also been reported to exhibit high liver and kidney uptake, radioactivity was cleared from these organs within a few hours (20-22). For example, in rats administered  $^{125}\text{I}$ -labeled hEGF, >90% of liver radioactivity was cleared within 90 minutes (19). In contrast, the concentration of  $^{111}\text{In}$  radioactivity in the liver and kidneys of mice administered  $^{111}\text{In}$ -DTPA-hEGF or  $^{111}\text{In}$ -DTPA-mAb 528 remained relatively constant up to 72 hours post-injection (Fig. 1). The clearance of radioactivity from the liver and kidneys following administration of  $^{125}\text{I}$ -labeled hEGF is thought to be due to binding of the radioligand to cell surface receptors on hepatocytes or renal tubular cells followed by internalization and degradation to free  $^{125}\text{I}$  and  $^{125}\text{I}$ -iodotyrosine. These catabolites are then exported from the cells and eliminated (23).  $^{111}\text{In}$ -DTPA-hEGF may follow a similar biological pathway involving its binding and internalization by hepatocytes or renal tubular cells and its degradation by intracellular proteases. However, in the case of  $^{111}\text{In}$ -DTPA-hEGF, the final catabolites are likely  $^{111}\text{In}$ -DTPA covalently linked to one of the two lysine residues ( $K_{28}$  or  $K_{48}$ ) or to the N-terminal asparagine. These terminal catabolites would not be recognized by amino acid

transporters and therefore would be retained within the cells (24).  $^{111}\text{In}$ -DTPA-mAb 528 may undergo a similar catabolic fate as  $^{111}\text{In}$ -DTPA-hEGF through its specific binding to cell surface receptors followed by internalization and degradation to catabolites which are retained by cells. Binding of  $^{111}\text{In}$ -DTPA-mAb 528 to hepatocytes could be mediated by binding to EGF receptors and also to Fc receptors (25).

Since hEGF is a peptide, it is readily filtered at the glomerulus and excreted into the urine.  $^{125}\text{I}$ -labeled EGF is cleared from the blood by glomerular filtration and is secreted by the proximal renal tubules following binding to receptors on renal tubular cells (26-28).  $^{125}\text{I}$ -labeled EGF is not reabsorbed by the renal tubules (28). It is likely that  $^{111}\text{In}$ -labeled hEGF is excreted by a similar mechanism. Renal excretion was the major factor which resulted in the rapid decrease in the blood concentration of  $^{111}\text{In}$ -DTPA-hEGF, since sequestration by the liver and kidneys accounted for only 11-14% and 4-5% of the injected dose of the radiopharmaceutical respectively.

Although there was a relatively high accumulation of the radiopharmaceuticals by normal tissues such as the liver and kidneys, both  $^{111}\text{In}$ -DTPA-hEGF and  $^{111}\text{In}$ -DTPA-mAb 528 localized sufficiently in the MDA-MB-468 and JW-97 human breast cancer xenografts to visualize the tumor at 72 hours post-injection by gamma scintigraphy (Fig. 3 and Fig. 4). The images obtained with  $^{111}\text{In}$ -DTPA-hEGF and  $^{111}\text{In}$ -DTPA-mAb 528 also showed relatively high normal tissue uptake by the liver and kidneys for the reasons discussed above, as well as localization of radioactivity in the area of the submaxillary glands. The normal liver and kidney accumulation of both radiopharmaceuticals could limit their clinical usefulness for the detection of liver or adrenal gland metastases in breast cancer patients. The submaxillary glands are responsible for EGF synthesis (29) and it is possible that receptors may be present in these tissues to bind and store the newly synthesized growth factor. EGF conjugated with other radionuclides has also been shown to localize in EGFR-positive tumors. Capala et al. (30) showed that  $^{99\text{m}}\text{Tc}$ -EGF was selectively retained in the brains of rats inoculated with glioma cells transfected with the EGFR gene but not in normal rats. Rusckowski et al. (31) imaged A431 squamous cell carcinoma xenografts ( $2 \times 10^6$  EGFR/cell) hosted in athymic mice with  $^{99\text{m}}\text{Tc}$ -EGF achieving tumor/blood ratios of 4:1 at 12 hours post injection. Cuartero-Plaza et al. (32) detected squamous cell lung carcinoma in 6/9 cancer patients by gamma scintigraphy using  $^{131}\text{I}$ -EGF. To our knowledge however, this is the first report of successful imaging of EGFR-positive human breast cancer using  $^{111}\text{In}$ -labeled EGF or anti-EGFR mAb 528.

The level of accumulation of  $^{111}\text{In}$ -DTPA-mAb 528 (11-22% i.d./g, Fig. 1-B) in the MDA-MB-468 and JW-97 tumors was 7 to 10 fold higher than that observed for  $^{111}\text{In}$ -DTPA-hEGF, allowing much clearer definition of the tumor despite the slightly lower tumor/blood ratios associated with  $^{111}\text{In}$ -DTPA-mAb 528

(5:1 versus 12:1, Fig. 2). Goldenberg et al. (33) successfully imaged MDA-MB-468 human breast cancer xenografts using the anti-EGFR mAb 225 (IgG<sub>2a</sub>) labeled with <sup>111</sup>In, but the tumor uptake was more than 5-fold lower than we observed with <sup>111</sup>In-labeled mAb 528 (4 versus 22 % i.d./g). Since <sup>111</sup>In labeled mAb 225 has already been shown to successfully image squamous cell lung carcinoma in cancer patients (34), the higher tumor uptake observed with <sup>111</sup>In-DTPA-mAb 528 in the MDA-MB-468 human breast cancer xenograft model in our study, is encouraging for the ultimate clinical application of this new radiopharmaceutical for the diagnostic imaging of EGFR-positive breast cancer in humans.

It is interesting to speculate why we observed no direct quantitative relationship between the level of receptors measured on the breast cancer cell lines *in vitro* and the level of accumulation of either radiopharmaceutical in the corresponding breast cancer xenografts *in vivo*. This finding was not due to the inactivation of either hEGF or mAb 528 upon radiolabeling with <sup>111</sup>In, since cell binding assays demonstrated that both radiopharmaceuticals exhibited their expected receptor binding properties (Table 1). Furthermore, biodistribution studies in animals bearing MDA-MB-468 breast cancer xenografts administered a non-specific <sup>111</sup>In-labeled IgG<sub>2a</sub> or <sup>111</sup>In-DTPA-hEGF mixed with an excess of non-radioactive hEGF (to compete with radiolabeled hEGF for receptor binding) demonstrated a 2 to 5-fold decrease in tumor uptake, suggesting that the tumor accumulation of the radiopharmaceuticals was receptor-mediated.

One possible explanation for our inability to observe a direct correlation between receptor expression levels *in vitro* and tumor uptake of the radiopharmaceuticals *in vivo*, is that in the context of tumor-bearing mice, only very small concentrations of the radiopharmaceuticals actually reached the interstitial fluid bathing the cancer cells. Under these conditions, the concentration of EGF receptors on the breast cancer cells may have been in excess and the amount of radioligand was therefore the limiting factor which controlled tumor uptake. For example, based on a tumor uptake of ~2% i.d./g (Fig. 1) and an injected dose of 1 mg of <sup>111</sup>In-DTPA-hEGF, there would be approximately  $2 \times 10^{12}$  molecules of the radiopharmaceutical (0.02 mg) delivered to  $2.5 \times 10^8$  MDA-MB-468 breast cancer cells contained in a 1 g breast cancer xenograft (assuming a breast cancer cell with a diameter of 20  $\mu$ m). The cells would express a total of  $2.5 \times 10^{14}$  EGFR at an expression level of  $\sim 10^6$  EGFR/cell (Table 1) and therefore, there would be about a 100-fold excess of receptors present in the tumor compared to the radioligand. Similarly, for <sup>111</sup>In-DTPA-mAb 528, assuming an injected dose of 50 mg and a tumor uptake of 15% i.d./g (Fig. 1), there would be approximately  $3 \times 10^{13}$  molecules (7.5 mg) of mAb 528 delivered to the tumor. In this case, there would be a 10-fold excess of receptors compared to radioligand. The receptor level on the breast cancer cells was measured *in vitro* by increasing the concentration of radioligand until the

concentration of receptors on the cells was the limiting factor. Under these conditions, breast cancer cells with a lower level of receptor expression (eg. MCF-7 cells) bound less radioligand than cells with a higher level of receptor expression (eg. MDA-MB-468 cells).

Although, the range of EGFR expression levels on the tumor xenografts studied was not as wide as that in our study, Rusckowski et al. (31) also recently noted a similar finding using  $^{99m}\text{Tc}$ -EGF in athymic mice bearing either A431 squamous cell carcinoma or LS174T colon cancer xenografts. Despite a 6-fold difference in EGFR expression *in vitro* between the A431 and LS174T cells ( $2 \times 10^6$  versus  $3.6 \times 10^5$  EGFR/cell respectively), there was no statistically significant difference in tumor uptake *in vivo* ( $0.4 \pm 0.09$  versus  $0.32 \pm 0.06$  % i.d./g respectively). Senekowitsch-Schmidtke et al. (35) found a partial correlation between tumor uptake and EGF receptor level in human tumor xenografts implanted into athymic mice using  $^{125}\text{I}$ -EGF but not with  $^{125}\text{I}$ -labelled anti-EGFR mAb 425. The tumor uptake of  $^{125}\text{I}$ -EGF was 2-fold higher in A431 xenografts compared to gastric cancer xenografts but the A431 tumors expressed an 8-fold higher level of EGF receptors. The tumor uptake of  $^{125}\text{I}$ -mAb 425 was higher in breast cancer xenografts than in A431 tumors despite higher EGFR expression by the A431 tumors. The results of our study suggest that the level of tumor localization of receptor-binding radiopharmaceuticals *in vivo* is controlled to a greater extent by their rate of elimination from the blood rather than by the level of receptor expression on cancer cells, provided that the radiopharmaceutical retains receptor binding capability and a minimal level of receptors is available for binding. An analogous inverse correlation has also been previously observed between the elimination rate and tumour accumulation of different forms of radiolabelled mAbs (eg. IgG vs.  $\text{F(ab')}_2$  vs. Fab') (25).

## CONCLUSIONS

In summary, the results of this study demonstrate that a direct quantitation of the level of receptor expression on cancer cells *in vivo* by gamma scintigraphy may not be possible. Nevertheless EGFR-positive tumor nodules in mice were detected qualitatively using radiopharmaceuticals which specifically bind to the receptor. Radiolabeled anti-EGFR mAbs would be more effective receptor-binding radiopharmaceuticals for tumor imaging in cancer patients than peptide-based agents such as hEGF, since their slower elimination rate from the blood leads to higher tumor uptake at only moderately lower tumor/blood ratios. Recent clinical studies with  $^{99m}\text{Tc}$ -anti-EGFR mAb ior egf/r3 have demonstrated that EGFR-positive lesions can be detected with high sensitivity in cancer patients (36).

## Acknowledgements

This research was supported in part by grants from DuPont Pharma, the Susan G. Komen Breast Cancer Foundation (Grant No. 9749) and the U.S. Army Breast Cancer Research Program (Grant No. DAMD17-98-1-8171) to R.M.R. and by a grant from the National Cancer Institute of Canada with funds from the Canadian Cancer Society to J.G. Parts of this study were presented at the Society of Nuclear Medicine, 45<sup>th</sup> Annual Meeting, Toronto, June 8, 1998.

## REFERENCES

1. Klijn JGM, Berns PMJJ, Schmitz PIM, and Foekens JA. The clinical significance of epidermal growth factor receptor (EGF-R) in human breast cancer: a review on 5232 patients. *Endocr Rev* 1992; 13:3-17.
2. Mendelsohn J. Epidermal growth factor receptor as a target for therapy with antireceptor monoclonal antibodies. *J Natl Cancer Inst Monogr* 1992; 13:125-131.
3. Fry DW, Kraker AJ, McMichael A, et al. A specific inhibitor of the epidermal growth factor receptor tyrosine kinase. *Science* 1994; 265:1093-1095.
4. Shaw JP, Akiyoshi DE, Arrigo DA, et al.. Cytotoxic properties of DAB<sub>486</sub>EGF and DAB<sub>389</sub>EGF, EGF receptor targeted fusion toxins. *J Biol Chem* 1991; 266:21118-21124.
5. Reilly R.M, Kiarash R, Cameron RG, et al.. Indium-111 labelled epidermal growth factor is selectively radiotoxic to human breast cancer cells overexpressing the epidermal growth factor receptor. *J Nucl Med* (in press) 1999.
6. Andersson A, Capala J, and Carlsson J. Effects of EGF-dextran-tyrosine-<sup>131</sup>I conjugates on the clonogenic survival of cultured glioma cells. *J Neuro Oncol* 1992; 14:213-223.
7. Kuukasjarvi T, Kononen J, Helin H and Isola J. Loss of estrogen receptor in recurrent breast cancer is associated with poor response to endocrine therapy. *J Clin Oncol* 1996; 14:2584-2589.
8. Fischman AJ, Babich JW and Strauss HW. A ticket to ride: peptide radiopharmaceuticals. *J Nucl Med* 1993; 34:2253-2263.

9. Gill GN, Kawamoto T, Cochet C, et al. Monoclonal anti-epidermal growth factor receptor antibodies which are inhibitors of epidermal growth factor binding and antagonists of epidermal growth factor-stimulated tyrosine protein kinase activity. *J Biol Chem* 1984; 259:7755-7760.
10. Filmus J, Trent JM, Pollak MN and Buick RN. Epidermal growth factor receptor gene-amplified MDA-468 breast cancer cell line and its non-amplified variants. *Molec Cellular Biol* 1987; 7:251-257.
11. Reilly RM and Gariépy J. Investigation of factors influencing the sensitivity of tumour detection using a receptor-binding radiopharmaceutical. *J Nucl Med* 1998; 39:1037-1042.
12. Reilly RM, Marks A, Law J, Lee NS and Houle S. *In-vitro* stability of EDTA and DTPA immunoconjugates of monoclonal antibody 2G3 labelled with In-111. *Appl Radiat Isot* 1992; 43:961-967.
13. Motulsky HJ, Stannard P and Neubig R. *Prism Ver 2.0*. San Diego, CA:GraphPad Software Inc.;1995.
14. Lindmo T, Boven E, Cuttitta F, Fedorko J and Bunn Jr. PA. Determination of the immunoreactive fraction of radiolabelled monoclonal antibodies by linear extrapolation of binding to infinite antigen excess. *J Immunol Meth* 1984; 72:77-89.
15. Dunn WA and Hubbard AL. Receptor-mediated endocytosis of epidermal growth factor by hepatocytes in the perfused rat liver: ligand and receptor dynamics. *J Cell Bio*. 1984; 98:2148-2159.
16. Gladhaug P and Christoffersen T. Kinetics of epidermal growth factor binding and processing in isolated intact rat hepatocytes: Dynamic externalization of receptors during ligand internalization. *Eur J Biochem* 1987; 164:267-275.
17. Yanai S, Sugiyama Y, Kim DC, et al. Binding of human epidermal growth factor to tissue homogenates of the rat. *Chem Pharm Bull* 1987; 35:4891-4897.
18. Fisher DA, Salido EC and Barajas L. Epidermal growth factor and the kidney. *Annu Rev Physiol* 1989; 51:67-80.
19. St.Hilaire RJ, Hradek GT and Jones AL. Hepatic sequestration and biliary secretion of epidermal growth factor: Evidence for a high-capacity uptake system. *Proc Natl Acad Sci USA* 1983; 80:3797-3801.

20. De Acosta CM, Justiz E, Skoog L and Lage A. Biodistribution of radioactive epidermal growth factor in normal and tumor bearing mice. *Anticancer Res* 1989; 9:87-92.
21. Scott-Robson S, Capala J, Carlsson J, et al. Distribution and stability in the rat of a  $^{76}\text{Br}/^{125}\text{I}$ -labelled polypeptide, epidermal growth factor. *Nucl Med Biol* 1991; 18:241-246.
22. Vinter-Jensen L, Frokiaer J, Jorgensen PE, et al. Tissue distribution of  $^{131}\text{I}$ -labelled epidermal growth factor in the pig visualized by dynamic scintigraphy. *J Endocrinol* 1995; 144:5-12.
23. Tyson LM, Browne CA, Jenkin G and Thorburn GD. The fate and uptake of murine epidermal growth factor in the sheep. *J Endocrinol* 1989; 123:121-130.
24. Duncan JR and Welch MJ. Intracellular metabolism of indium-111-DTPA labeled receptor targeted proteins. *J Nucl Med* 1993; 34:1728-38.
25. Reilly RM, Sandhu J, Alvarez-Diez T, et al. Problems of delivery of monoclonal antibodies: Pharmaceutical and pharmacokinetic solutions. *Clin Pharmacokinet* 1995; 28:126-142.
26. Kim DC, Sugiyama Y, Fuwa T, et al. Kinetic analysis of the elimination process of human epidermal growth factor (hEGF) in rats. *Biochem Pharmacol* 1989; 38:241-249.
27. Jorgensen PE, Poulson SS and Nexø E. Distribution of i.v. administered epidermal growth factor in the rat. *Regulatory Peptides* 1988; 23:161-169.
28. Nielsen S, Nexø E, and Christensen EI. Absorption of epidermal growth factor and insulin in rabbit renal proximal tubules. *Am J Physiol* 1989; 256:E55-E63.
29. Carpenter G and Cohen S. Epidermal growth factor. *Ann Rev Biochem* 1979; 48:193-216.
30. Capala J, Barth RF, Bailey MQ, Fenstermaker RA, Marek M and Rhodes, B.A. Radiolabeling of epidermal growth factor with  $^{99\text{m}}\text{Tc}$  and *in vivo* localization following intracerebral injection into normal and glioma-bearing rats. *Bioconjugate Chem* 1997; 8:289-295.

31. Rusckowski M, Qu T, Chang F and Hnatowich DJ. Technetium-99m labeled epidermal growth factor-tumor imaging in mice. *J Peptide Res* 1997; 50:393-401.
32. Cuartero-Plaza A, Martinez-Miralles E, Rosell R, Vadell-Nadal C, Farre M and Real, FX. Radiolocalization of squamous lung carcinoma with <sup>131</sup>I-labeled epidermal growth factor. *Clin Cancer Res* 1996; 2:13-20.
33. Goldenberg A, Masui H, Divgi C, et al. Imaging of human tumor xenografts with an indium-111-labeled anti-epidermal growth factor receptor monoclonal antibody. *J Natl Cancer Inst* 1989; 81:1616-1625.
34. Divgi CR, Welt S and Kris M. Phase I and imaging trial of indium-111 labeled anti-EGF receptor monoclonal antibody 225 in patients with squamous cell lung carcinoma. *J Natl Cancer Inst* 1991; 83:97-104.
35. Senekowitsch-Schmidtke R, Steiner K, Haunschild J, Mollenstadt S and Truckenbrodt R. In vivo evaluation of epidermal growth factor (EGF) receptor density on human tumor xenografts using radiolabeled EGF and anti-(EGF receptor) mAb 425. *Cancer Immunol Immunother* 1996; 42:108-114.
36. Ramos-Suzarte M, Rodríguez N, Oliva JP et al. <sup>99m</sup>Tc-labeled antihuman epidermal growth factor receptor antibody in patients with tumors of epithelial origin: Part III. Clinical trials safety and diagnostic efficacy. *J Nucl Med* 1999; 40:768-775.

## LEGENDS FOR FIGURES

**FIGURE 1.** Biodistribution at selected times post i.v. administration of  $^{111}\text{In}$ -DTPA-hEGF (A) and  $^{111}\text{In}$ -DTPA-mAb 528 (B) in athymic mice bearing s.c. MDA-MB-468 human breast cancer xenografts. Tissues shown are blood (B), heart (H), lungs (Lu), liver (L), kidneys (K), spleen (Sp), stomach (S), intestines (I) and tumor (T).

**FIGURE 2.** Tumour/normal tissue ratios at selected times post i.v. administration of  $^{111}\text{In}$ -DTPA-hEGF (A) and  $^{111}\text{In}$ -DTPA-mAb 528 (B) in athymic mice bearing s.c. MDA-MB-468 human breast cancer xenografts. Tissues shown are blood (B), heart (H), lungs (Lu), liver (L), kidneys (K), spleen (Sp), stomach (S) and intestines (I).

**FIGURE 3.** Posterior whole body images of an athymic mouse bearing a s.c. MDA-MB-468 human breast cancer xenograft at 72 hours post-injection of  $^{111}\text{In}$ -DTPA-hEGF (A) or  $^{111}\text{In}$ -DTPA-mAb 528 (B). The tumor is visualized with either radiopharmaceutical but is more clearly defined with  $^{111}\text{In}$ -DTPA-mAb 528.

**FIGURE 4.** Posterior whole body images of a *scid* mouse bearing a s.c. JW-97 human breast cancer xenograft at 72 hours post-injection of  $^{111}\text{In}$ -DTPA-hEGF (A) or  $^{111}\text{In}$ -DTPA-mAb 528 (B). The tumor is visualized with either radiopharmaceutical but is more clearly defined with  $^{111}\text{In}$ -DTPA-mAb 528.

TABLE 1

Comparison of binding of  $^{111}\text{In}$  and  $^{125}\text{I}$  labeled human epidermal growth factor or monoclonal antibody 528 to MDA-MB-468 human breast cancer cells.

	$^{111}\text{In}$ -DTPA-hEGF	$^{125}\text{I}$ -hEGF	$^{111}\text{In}$ -DTPA-mAb 528	$^{125}\text{I}$ -mAb 528
n	6	10	5	4
$K_a$ (L/mol)*	$7.5 \pm 3.8 \times 10^8$	$7.3 \pm 3.6 \times 10^8$	$1.2 \pm 0.6 \times 10^8$	$9.4 \pm 2.0 \times 10^7$
$B_{\text{max}}$ (Sites/cell)*	$1.3 \pm 0.3 \times 10^6$	$7.2 \pm 0.3 \times 10^5$	$9.0 \pm 4.5 \times 10^5$	$7.0 \pm 3.8 \times 10^5$

\* Affinity constant (Mean  $\pm$  S.D.).

† Maximum number of binding sites/cell (Mean  $\pm$  S.D.)

TABLE 1

Comparison of binding of  $^{111}\text{In}$  and  $^{125}\text{I}$  labeled human epidermal growth factor or monoclonal antibody 528 to MDA-MB-468 human breast cancer cells.

	$^{111}\text{In}$ -DTPA-hEGF	$^{125}\text{I}$ -hEGF	$^{111}\text{In}$ -DTPA-mAb 528	$^{125}\text{I}$ -mAb 528
n	6	10	5	4
$K_a$ (L/mol)*	$7.5 \pm 3.8 \times 10^8$	$7.3 \pm 3.6 \times 10^8$	$1.2 \pm 0.6 \times 10^8$	$9.4 \pm 2.0 \times 10^7$
$B_{\text{max}}$ (Sites/cell)*	$1.3 \pm 0.3 \times 10^6$	$7.2 \pm 0.3 \times 10^5$	$9.0 \pm 4.5 \times 10^5$	$7.0 \pm 3.8 \times 10^5$

\* Affinity constant (Mean  $\pm$  S.D.).

† Maximum number of binding sites/cell (Mean  $\pm$  S.D.)

*Figures available on request.*

heated with (But)<sub>4</sub>NF in EtOAc at 70°C for 20 min. The *arabino* fluorosugar was characterized by spectroscopic methods (NMR and MS). Radiochemical syntheses were performed with F-18 fluoride. F-18 fluoride was reacted with (But)<sub>4</sub>NHCO<sub>3</sub> and evaporated to dryness. The dry (But)<sub>4</sub>NF was dissolved in THF and heated with the 2-O-fluorosulfonyl derivative in EtOAc. The crude product was purified by HPLC. **Results:** The average radiochemical yield was 19% in 11 runs, with radiochemical purity >99%. Specific activities were 4.4-9.3 GBq/μmole. Synthesis time was 75-80 min from EOB. **Conclusion:** The arabinofuranose was successfully labeled with F-18 and may be a useful intermediate for synthesis of nucleoside analogues for PET.

# No. 1369

**TUMOR LOCALIZATION OF TC-99M LABELED 5-THIO-D-GLUCOSE (TG).** K. S. Ozker\*, B. D. Collier, D. J. Lindner, A. Z. Krasnow, R. S. Hellman, Y. Liu, L. Kabasakal, D. S. Edwards, C. R. Bourque, P. D. Crane, Medical College of Wisconsin, Milwaukee, WI; University of Maryland, Baltimore, MD; Cerrahpasa Medical School, Istanbul, Turkey; DuPont Merck Pharmaceutical Company, North Billerica, MA. (101093)

**Objectives.** Recent studies attest to the avidity of Tc-99m labeled carbohydrate ligands (glucuronate and gluconate) for tumors and sites of acute ischemic injury. The exact mechanism of localization for Tc-99m labeled carbohydrate ligands is currently not known. The purpose of this work is to study the pattern of tumor localization of a Tc-99m labeled carbohydrate ligand, Tc-99m-TG. TG, an analog of D-glucose, binds to Tc-99m via a thio substitute. **Methods.** Biodistribution studies of Tc-99m-TG administered to mice bearing MC26 colon carcinoma in their thigh was used to determine the tumor localization and tumor to BG (normal muscle from contralateral thigh) ratios. Autoradiography of Tc-99m-TG was also compared to that of C-14 labeled 2-deoxyglucose (C-14-DG) in a subgroup of mice. **Results.** Tumor uptake of Tc-99m-TG was  $1.6 \pm 0.3\%$  ID/g at 1 hour which decreased slightly to  $1.3 \pm 0.3\%$  ID/g and  $1.2 \pm 0.3\%$  ID/g at 2 and 3 hours post-injection respectively. However, tumor to BG ratio exhibited a significant increase between 1 and 3 hours (2.7/1 and 4/1), due to gradually decreasing body BG. Tumor autoradiography of Tc-99m-TG and C-14-DG showed different patterns of localization. Tc-99m-TG concentrated at the center of the tumors while C-14-DG had decreased activity in this central area, suggesting Tc-99m-TG avidity to zones of infarction/necrosis and C-14-DG avidity to viable tumor cells in the periphery. **Conclusion.** Results of this study indicate that Tc-99m-TG exhibits increased tumor localization and T/BG ratio. The discordance between tumor localization of Tc-99m-TG and C-14-DG suggests that Tc-99m-TG does not act like a glucose analog and warrants further investigation as an imaging agent for areas of necrosis.

# No. 1370

**PRODUCTION OF A HUMAN EPIDERMAL GROWTH FACTOR (hEGF)-IMMUNOGLOBULIN (C<sub>1</sub>) FUSION PROTEIN FOR TARGETING HUMAN BREAST CANCER.** J. Wang\*, J. Sandhu, Z. Chen, C. Leung, M. Bray, S. Yang, R. Cameron, A. Hendler, K. Vallis, R. M. Reilly, The Toronto Hospital, Toronto, ON, Canada; Samuel Lunenfeld Research Institute, Toronto, ON, Canada; Ontario Cancer Institute, Toronto, ON, Canada; Princess Margaret Hospital, Toronto, ON, Canada; The Toronto Hospital/University of Toronto, Toronto, ON, Canada. (100173)

Overexpression of the EGF receptor (EGFR) occurs in 30-60% of breast cancers. Preliminary studies showed that In-111 hEGF localized specifically in MDA-468 human breast cancer xenografts (>10<sup>6</sup> EGFR/cell) in nude mice (tumour/blood ratio >12:1) but tumour uptake was low (2-3% i.d./g). Tumour uptake of hEGF (m.w. 6 kDa) could possibly be improved by slowing its renal elimination by fusion with a macromolecule. **Objective:** To produce an hEGF fusion protein consisting of hEGF and the C<sub>1</sub> domain of IgG<sub>1</sub> to more effectively target radionuclides to EGFR-positive breast cancer. **Methods:** The gene for hEGF (*pADH59*) was fused with the gene for C<sub>1</sub> of mIgG<sub>1</sub> (*pASK84*) with/without a peptide linker sequence [(GGGGG)<sub>3</sub>] and inserted into expression vector *pGEX2T*. *E. coli* (BL21) were transformed with the *p-hEGF-C<sub>1</sub>* expression vector and ampicillin-resistant colonies grown to produce a hEGF-C<sub>1</sub> glutathione S-transferase (GST) fusion protein. GST-hEGF-C<sub>1</sub> protein was extracted under native conditions and purified on a glutathione-Sepharose column. GST-hEGF-C<sub>1</sub> was assessed for purity by SDS-PAGE and Western blot with a polyclonal anti-EGF antibody and

for receptor binding by ELISA and flow cytometry. **Results:** GST-hEGF-C<sub>1</sub> protein was obtained in high yield (1 mg/L). SDS-PAGE showed a single band (m.w. 44 kDa) positive for hEGF by Western blot. GST-hEGF-C<sub>1</sub> exhibited strong binding by ELISA to EGFR isolated from MDA-468 breast cancer cells and to live A431 cells by flow cytometry. **Conclusion:** An hEGF-C<sub>1</sub> fusion protein with preserved receptor-binding properties was produced in high yield and purity. Experiments are planned to evaluate the hEGF-C<sub>1</sub> protein labelled with In-111 for targeting MDA-468 breast cancer xenografts in nude mice. Supported by Susan G. Komen Breast Cancer Foundation and US Army BCRP.

# No. 1371

**ENHANCED ACCUMULATION OF ALBUMIN IN INTRAPERITONEAL TUMORS FOLLOWING MANNOSYLATION.** Z. Yao\*, M. Zhang, H. Sakahara, Y. Arano, H. Saji, J. Konishi, Clinical Center, The National Institutes of Health, Bethesda, MD; Kyoto University, Kyoto, Japan. (500312)

We have shown that glycosylation of avidin is one of the important factors of its tumor accumulation. This study was undertaken to investigate the potential of glycosylated albumin in targeting intraperitoneal (i.p.) tumor xenografts. Three tumor xenograft models, including a colon cancer, LS180, an ovarian cancer, SHIN-3, and a gastric cancer, MKN45, were established by i.p. injections of the human cancer cells in nude mice. Human serum albumin (HSA) was conjugated with galactose or mannose. Galactosyl-neoglycoalbumin (NGA), mannosyl-neoglycoalbumin (NMA), or HSA was labeled with In-111 through SCN-Bz-EDTA conjugation. The radiolabeled proteins were administered i.p. into the tumor-bearing mice and the biodistribution of radioactivity was examined at 2 and 24 hours postinjection. The results show that glycosylation of albumin increased blood clearance and liver accumulation of radioactivity. Tumor uptake was significantly increased with NMA, resulting in a high tumor-blood ratio. NGA accumulated in tumors higher than HSA but much lower than NMA. Similar biodistribution pattern of radioactivity was also observed 24 hour postinjection. The biodistribution in SHIN-3 or MKN45 tumor-bearing mice was similar to that in LS180. In conclusion, mannosyl glycosylation of albumin enhanced its accumulation in i.p. tumors when administered i.p.. The high targeting efficiency could make NMA a useful vehicle for the delivery of radionuclide or other therapeutic agents to i.p. tumors for the diagnosis and therapy.

Biodistribution of radioactivity in mice bearing LS180 xenograft (%ID/g, 2 h)

	HSA	NGA	NMA
Blood	8.50±2.75	0.28±0.23	0.30±0.08
Liver	2.97±0.75	18.31±6.49	12.95±2.98
Tumor	3.61±0.75	6.17±1.12	19.31±4.07

# No. 1372

**SYNTHESIS AND CHARACTERISATION OF I-123- AND I-125-DIETHYLSTILBESTROL (DES) WITH HIGH SPECIFIC ACTIVITY.** K. Schomaecker, T. Fischer\*, H. Schmickler, B. Meller, B. Gabruk-Szostak, H. Schicha, Clinic of Nuclear Medicine, University of Cologne, Cologne, Germany; University of Cologne/Institute of Organic Chemistry, Cologne, Germany; Department of Nuclear Medicine, University of Luebeck, Luebeck, Germany. (100073)

**Rationale:** Radioactive labeled DES is an interesting compound for therapy of estrogen receptor (ER)-positive mamma-carcinoma. Until now, labeling procedures suffered from low yields (20 - 30%) with low specific activities (0.74 - 2.96 GBq/mmol) and bad reproducibility. **Aims:** a) Development of a simple and fast labeling method for \*I-DES with high yield and specific activity b) Structure analysis by NMR c) Determination of the dissociation constant. **Methods:** a) Labeling was done with chloramine T in methanol within 10 min at room temperature. Purification was performed with RP-HPLC. For NMR experiments, synthesis was done with stable iodine, followed by preparative HPLC. b) For structure analysis <sup>1</sup>H-NMR, <sup>13</sup>C-NMR, H,H-COSY and HMBC were used. c) Dissociation constant was determined by incubation of ER-positive tumor cytosol with varied <sup>125</sup>I-DES amounts, with and without additional DES, followed by a Scatchard plot. **Results:** a) \*I-DES was produced with yields of 50 - 70% and specific activity of 80 TBq/mmol. b) Some of the reaction products could be identified and the structure of I-DES was verified. 3-iodo-DES and 2-iodo-DES were found in a 8.5/1 ratio. c) The dissociation con-



DEPARTMENT OF THE ARMY  
US ARMY MEDICAL RESEARCH AND MATERIEL COMMAND  
504 SCOTT STREET  
FORT DETRICK, MD 21702-5012

REPLY TO  
ATTENTION OF

MCMR-RMI-S (70-1y)

15 May 03

MEMORANDUM FOR Administrator, Defense Technical Information  
Center (DTIC-OCA), 8725 John J. Kingman Road, Fort Belvoir,  
VA 22060-6218


SUBJECT: Request Change in Distribution Statement

1. The U.S. Army Medical Research and Materiel Command has reexamined the need for the limitation assigned to technical reports written for this Command. Request the limited distribution statement for the enclosed accession numbers be changed to "Approved for public release; distribution unlimited." These reports should be released to the National Technical Information Service.

2. Point of contact for this request is Ms. Kristin Morrow at DSN 343-7327 or by e-mail at Kristin.Morrow@det.amedd.army.mil.

FOR THE COMMANDER:

Encl

  
PHYLIS M. RINEHART  
Deputy Chief of Staff for  
Information Management

ADB266022	ADB265793
ADB260153	ADB281613
ADB272842	ADB284934
ADB283918	ADB263442
ADB282576	ADB284977
ADB282300	ADB263437
ADB285053	ADB265310
ADB262444	ADB281573
ADB282296	ADB250216
ADB258969	ADB258699
ADB269117	ADB274387
ADB283887	ADB285530
ADB263560	
ADB262487	
ADB277417	
ADB285857	
ADB270847	
ADB283780	
ADB262079	
ADB279651	
ADB253401	
ADB264625	
ADB279639	
ADB263763	
ADB283958	
ADB262379	
ADB283894	
ADB283063	
ADB261795	
ADB263454	
ADB281633	
ADB283877	
ADB284034	
ADB283924	
ADB284320	
ADB284135	
ADB259954	
ADB258194	
ADB266157	
ADB279641	
ADB244802	
ADB257340	
ADB244688	
ADB283789	
ADB258856	
ADB270749	
ADB258933	